

MECHANISM OF ACTION OF NICOTINAMIDE PHOSPHORIBOSYLTRANSFERASE  
MEDIATED SIGNALING IN OXIDATIVE STRESS

A DISSERTATION IN  
Cell Biology and Biophysics  
and  
Molecular Biology and Biochemistry

Presented to the Faculty of the University  
of Missouri-Kansas City in partial fulfillment of  
the requirements for the degree

DOCTOR OF PHILOSOPHY

by  
Bryan Gerdes

M.S., University of Missouri-Kansas City, Kansas City, MO 2014  
B.S., Kansas State University, Manhattan, KS 2008  
B.S., Kansas State University, Manhattan, KS 2006

Kansas City, MO  
2018

© 2018

Bryan Christopher Gerdes

ALL RIGHTS RESERVED

MECHANISM OF ACTION OF NICOTINAMIDE PHOSPHORIBOSYLTRANSFERASE  
MEDIATED SIGNALING IN OXIDATIVE STRESS

Bryan Christopher Gerdes, Candidate for the Doctor of Philosophy Degree

University of Missouri-Kansas City, 2018

ABSTRACT

Worldwide there are an estimated 1 billion people that are affected by a form of neurodegenerative disease. The most common forms of neurodegenerative disease are Alzheimer's disease and Parkinson's disease, along with diseases that are attributed to damage of the retina and optic nerve, such as macular degeneration and glaucoma. Nearly five million people have been diagnosed with Alzheimer's disease in the United States of America alone (1). Another disease that effects 4 million people in the US is glaucoma, and it is the second most common form of blindness after age-related macular degeneration (AMD) (2). Alzheimer's disease, AMD, and glaucoma are all neurodegenerative diseases that are caused by oxidative stress. Neuroprotection and protection of cells supporting the function of neurons could provide novel therapeutic approaches to treating and preventing neurodegenerative diseases when therapies do not exist or existing therapies fail (3).

Nicotinamide phosphoribosyltransferase (Nampt) is an enzyme critical for cellular energy metabolism, and it also functions as a proinflammatory cytokine and growth factor with neuroprotective properties and in these contexts is referred to as Pre-B-Cell Colony Enhancing Factor (PBEF) and Visfatin, respectively. Nampt/PBEF/Visfatin has been

implicated in a number of human diseases, including acute lung injury, rheumatoid arthritis, vascular disorders, and diabetes. Based on previous evidence suggesting a protective role of Nampt/PBEF/Visfatin in ischemia, the hypothesis was tested that Nampt/PBEF/Visfatin exerts protective effects against oxidative stress in established *in vitro* models of neurodegeneration and of cellular degeneration related to neurodegenerative diseases.

The PBEF gene was cloned into a prokaryotic expression vector, recombinantly expressed as a Glutathione-S-transferase-fusion protein, and purified by affinity chromatography. Optimization of a fluorescent enzyme activity assay was performed in order to quantify the Nampt/PBEF/Visfatin-mediated conversion of nicotinamide to nicotinamide mononucleotide, confirming enzymatic activity of recombinant Nampt/PBEF/Visfatin *in vitro*. Testing of neuroprotective properties of recombinant Nampt/PBEF/Visfatin was conducted in the human neuroblastoma cell line SH-SY5Y using the calcein-acetomethoxy ester uptake assay, which measures cellular viability. Testing of siRNA transfection mediated knockdown of endogenous Nampt was performed in the retinal pigment epithelial cell line ARPE-19 and primary isolated optic nerve head astrocytes as models for cells supporting the viability and function of retinal neurons. The use of siRNA in both ARPE-19 and ONHA cell lines demonstrated how the loss of endogenous Nampt affected each cell line when treated with tBHP. Visual cell counts were performed after knockdown of Nampt and treatment of tBHP, and rNampt was used as a neuronal protective in order to produce cellular recovery.

Recombinant Nampt/PBEF/Visfatin was enzymatically active and applied to each cell type extracellularly in the pre-treatment stage when fresh media was added to the cells. This addition of rNampt reduced cell death resulting from chemically induced oxidative stress *in*

*vitro* by approximately 25% in SH-SY5Y cell line. Similar results were seen in both ARPE-19 cells and ONHA when oxidative stress was induced by ROS. Removal of endogenous Nampt by pharmacological inhibition or siRNA-mediated knockdown had no effect on general cell viability but cell lines ARPE-19 and ONHA became more sensitive to oxidative stress and cells entered apoptosis earlier than WT. After knockdown of endogenous Nampt cells were pre-treated with rNampt and shown to have increased cell survival from neuronal protection from oxidative stress. An improved understanding of the mechanisms of action underlying Nampt/PBEF/Visfatin-mediated neuro- and cellular protection has the potential to contribute to the development of new therapies to treat neurodegenerative diseases.

## APPROVAL PAGE

The faculty listed below, appointed by the Dean of the School of Graduate Studies, have examined a dissertation titled, “Mechanism of Action of Nicotinamide Phosphoribosyltransferase Mediated Signaling in Oxidative Stress”, presented by Bryan Christopher Gerdes, candidate for the Doctor of Philosophy degree, and certify that in their opinion it is worthy of acceptance.

### Supervisory Committee

Peter Koulen, Ph.D., Committee Chair  
Cell Biology and Biophysics

Thomas Menees, Ph.D.  
Cell Biology and Biophysics

Jeffrey Price, Ph.D.  
Molecular Biology and Biochemistry

Ann Smith, Ph.D.  
Molecular Biology and Biochemistry

Anthony Persechini, Ph.D.  
Molecular Biology and Biochemistry

## TABLE OF CONTENTS

ABSTRACT.....	iii
LIST OF FIGURES.....	xiii
LIST OF TABLES.....	ix
LIST OF ABBREVIATIONS.....	x
ACKNOWLEDGEMENTS.....	xi
Chapter	
1. INTRODUCTION.....	1
2. MATERIALS AND METHODS.....	10
3. RESULTS.....	20
4. DISCUSSION.....	41
5. FUTURE DIRECTIONS.....	47
REFERENCES.....	48
VITA.....	57

## LIST OF FIGURES

Figure	Page
1. Expression of human recombinant Nampt (rNampt) protein.....	20
2. Conversion of Nicotinamide to fluorescent Nicotinamide mononucleotide derivative.....	21
3. Neuroprotective properties of rNampt in the neuronal SH-SY5Y cells.....	23
4. Neuroprotective properties of rNampt in ARPE-19 cells undergoing oxidative stress.....	25
5. Optimization of Nampt knockdown using siRNA in ARPE-19 cells.....	28
6. Knockdown of Nampt in ARPE-19 cells using siRNA .....	31
7. Optimization of Nampt knockdown using siRNA in ONHA cells.....	35
8. Knockdown of Nampt in ONHA cells using siRNA .....	38



## LIST OF TABLES

Table	Page
1. Each individual siRNA and its corresponding targeting sequence.....	28

## LIST OF ABBREVIATIONS

AD	Alzheimer's disease
APP	Amyloid precursor protein
Ca <sup>2+</sup>	Calcium ion
DMSO	Dimethyl sulfoxide
GFP	Green fluorescence protein
IPTG	Isopropyl $\beta$ -D-1-thiogalactopyranoside
mMs	Monoclonal antibody with mouse host
mRb	Monoclonal antibody with rabbit host
NAM	Nicotinamide
Nampt	Nicotinamide phosphoribosyltransferase
NMN	Nicotinamide mononucleotide
ONHA	Optic nerve head astrocyte
PBS	Phosphate buffered saline
PCR	Polymerase chain reaction
PS	Presenilin
pRb	Polyclonal antibody with rabbit host
pGt	Polyclonal antibody with rabbit host
RFU	Relative fluorescence unit
ROS	Reactive oxygen species
RyR	Ryanodine receptor

## ACKNOWLEDGEMENTS

Earning a doctorate and writing a dissertation can be a long and daunting experience, but it would not have been made possible without the opportunity, leadership, and support provided by Dr. Peter Koulen. I would also like to thank my dissertation committee members, Dr. Ann Smith, Dr. Jeffrey Price, Dr. Thomas Menees, and Dr. Anthony Persechini for all their support during graduate school. All of whom have provided great support and guided me through the process of completing my dissertation.

I want to extend special thanks to members of the lab that have given me great support throughout the years. Thanks to Dr. John Means for answering multiple questions and helping me navigate problems that arose. I owe a large debt to Dr. Simon Kaja and Dr. Andrew Pain who are no longer in the lab but provided a wealth of information and experience at the start of my project. I would like to say thank you to everyone in the School of Biological Sciences and everyone in the School of Graduate studies.

The support of my family and friends was an endless supply of encouragement and moral boost, all provided graciously to keep me going through troubled times. My parents Rick and Lisa Gerdes and Jonathan and Diane Morton, have given me excellent words of encouragement and endless conversations to help me push forward to pursue a higher education. My beautiful daughters Eva and Roselyn Gerdes, have always been a source of joy and light.

And in the end the person who was there the most and would never let me walk away was my fiancé Susan. Our lives have been a constant struggle and there has never been a moment when she wasn't there for me, reminding me of my dreams and why I started this

journey. Her sacrifices and support can never be repaid but after completion and during the celebrations she will know how much she was a part of this project.

## CHAPTER 1

### INTRODUCTION

#### **Effects of neurodegenerative diseases**

Neurodegenerative diseases are an increasing problem due to incurable and debilitating conditions that are a major concern to the healthcare of the world. The term neurodegenerative disease is used as a broad term to define diseases that affect neurons in the human brain(4). Neurons suffer progressive loss of structure or function to neurodegenerative diseases Parkinson's disease, Huntington's disease, and Alzheimer's disease. Such diseases are incurable resulting in progressive degeneration and death of neuronal cells. A form of neurodegenerative disease is one that involves misfolded proteins and aggregation of these proteins. These proteins include alpha-synuclein, prions, tau, and amyloid beta. Two diseases, Parkinson's and Huntington's disease, have the common feature of late-onset and intracellular toxic proteins buildup in either the cytosol, nucleus, or endoplasmic reticulum (5). Activation of a process called programmed cell death, or apoptosis, is an intracellular process that leads to cell death by activation of caspase proteins and morphology changes including cell blebbing, cell shrinkage, and nuclear fragmentation (3, 6, 7). Neurodegenerative diseases activate this process and cause cells to undergo cellular apoptosis. Neurodegenerative diseases vary but one common trait that they all share is increased levels of oxidative stress (8). The most common neurodegenerative diseases are similar in that oxidative stress is a cause of Alzheimer's disease and Parkinson's disease. Age-related macular degeneration (AMD) and glaucoma are retinal diseases that are caused by oxidative stress (9).

As the human population is living to older ages, dementia is a very common form of neurodegenerative diseases in the elderly population. Alzheimer's disease (AD) is a leading cause of dementia and a long-lasting form of neurodegenerative disease. Worldwide there are estimated 46.8 million people living with dementia, and AD is estimated to be the cause of around 50% of dementia cases (6, 7, 10-12) Alzheimer's disease not only a disease of old age, but can be seen in patients under the age of 65 suffering early-onset. Diagnosis of AD is confirmed with the presence of neurofibrillary tangles and amyloid plaques made up of the major component amyloid- $\beta$  ( $A\beta$ ) (13-16). Mutations have also been identified as an underlying cause of AD (17, 18). Mutations in the presenilin1 (PS1) and presenilin 2 (PS2) protein alter the amyloid precursor protein (APP) by increasing  $A\beta$  levels. With the mutation of PS1 and PS2 intracellular calcium signaling is altered and elevated calcium concentrations alter the  $Ca^{2+}$  homeostasis experienced during oxidative stress and can signal cellular apoptosis (19, 20).

Glaucoma affects a wide range of people by causing permanent blindness. Glaucoma alters the structure of the optic nerve, damages the visual field, and causes degeneration of retinal ganglion cells (RGCs) (21-24). Patients with glaucoma are diagnosed with either a high or abnormally higher intraocular pressure (IOP) leading to greater risk of eye damage. Higher IOP is produced when intraocular pressure is above 10 mm Hg and abnormal when IOP is greater than 21 mm Hg. Other factors can play a role in glaucoma such as nitric oxide, glutamate levels and oxidative damage from the presence of ROS (25-28). Glaucoma patients suffer from the continual loss of trabecular meshwork (TM) which has been linked to the effects of oxidative damage from free radicals (29, 30). Recent studies have been able to show that in humans the higher IOP

and damaged visual field correlate to oxidative damage within TM cells (31). Different diseases like cataracts, age-linked macular degeneration and glaucoma all contribute to the modification of eye structures by oxidative damage (32-34). Therapy is in place for glaucoma and has been shown to reduce IOP in some patients but not all have the same response. Neuroprotection in glaucoma would provide a way to prevent the loss of RGCs and damage to the optic nerve. New research on RGCs and neuroprotection against oxidative stress are currently being conducted in order to provide new forms of therapies for glaucoma.

Age-related macular degeneration (AMD) is a common eye condition where the retina is damaged and loss of retinal ganglion cells occurs. The macula, a small spot near the center of the retina, is damaged in AMD leading to vision loss because it is the part of the retina for sharp and central vision, although patients are able to keep peripheral vision (35). There are two forms of AMD: dry and wet. Dry form of AMD accounts for 80% of AMD cases and is diagnosed when the macula thins and the presence protein drusen under the retina. Vision is lost at a slow rate in dry AMD. Wet AMD occurs when blood vessels are seen growing underneath the retina. These vessels will leak fluids under the retina and cause damage to the macula. Vision is lost at a faster rate, and is unnoticeable until vision loss occurs (36). Oxidative stress was shown to be a major contributor to AMD by the Age-Related Eye Disease Study (AREDS), where smoking increased oxidative damage in patients with AMD (37). Oxidative stress has been shown to damage DNA specific for mitochondria in retinal pigment epithelium (RPE) cells in AMD (38). Protection against oxidative stress would provide a way to prevent loss of RPE cells and prevent disruption of energy production in mitochondria.

## **Current knowledge on and general overview of Nicotinamide phosphoribosyltransferase**

Nicotinamide phosphoribosyltransferase (Nampt)/pre-B-cell colony enhancing factor 1 (PBEF)/Visfatin are all the same protein but behave differently based on cellular location. It was named PBEF when first discovered to promote pre-B-cell colony formation in stem cells. Nampt was cloned from human peripheral blood lymphocytes in 1994 and Visfatin was discovered in 2005 by the identification of Visfatin mRNA from visceral adipose tissue, and is also an adipocyte hormone (30, 31, 39). This hormone has been seen in the cytoplasm and within organs including the brain, kidney, lung, spleen, and testis. This protein Pre-B-cell colony-enhancing factor 1 (PBEF1) is a cytokine involved in the maturation of B-cell precursors (39). Upregulation of PBEF1 by mechanical force and inflammatory stimuli has been shown in acute lung injury (40). Treatment of fetal membrane explants with PBEF1 resulted in upregulation of inflammatory cytokines TNF $\alpha$ , IL-6, and macrophage inflammatory proteins 1 $\alpha$ , 1 $\beta$ , and 3 $\alpha$  (41-43). The protein Nampt is a rate-limiting enzyme in the Nicotinamide adenine dinucleotide (NAD<sup>+</sup>) salvage pathway which regulates cellular NAD production (44). Cells that are damaged from disease have a higher energy demand than a non-damaged cell. Nampt also is a pro-inflammatory cytokine, and a growth factor that possesses neuroprotective properties against oxidative stress. Nampt has been implicated in a



number of human diseases, including acute lung injury, cerebral ischemia, rheumatoid arthritis, vascular disorders, and diabetes. Cerebral ischemia has been shown to lead to neuronal cell and brain damage when energy levels inside cells are exhausted (45). Cell death is seen to diminish when Nampt is present to increase conversion of NAM to NMN and maintain mitochondrial NAD levels (46). Suggesting a protective role of Nampt in ischemia, and it may exert protective effects against oxidative stress and prevent cell apoptosis. Intracellular  $\text{Ca}^{2+}$  concentrations control transcription, muscle contraction, cell proliferation, and cell survival, including the regulation of apoptosis (47, 48). It has been previously shown that oxidative stress causes an increase in  $\text{Ca}^{2+}$  levels disrupting energy metabolism and calcium homeostasis within a cell (45, 49).

### **Oxidative stress affects energy metabolism and calcium homeostasis**

#### **Calcium and ATP synthesis**

Mitochondrial ATP synthesis and cellular energy demand is a crucial balance within a cell. A cellular increase in energy demand requires an equal response in ATP synthesis to maintain ATP/ADP ratio. Synthesis of ATP is controlled by the electrochemical gradient on the inner mitochondrial membrane, with complex I, II, and IV producing the gradient and  $\text{Ca}^{2+}$  playing a critical role in signaling to activate mitochondrial ATP synthesis (50-53).

#### **Calcium homeostasis**

Calcium acts as an intracellular messenger that controls gene transcription, muscle contraction, and cell proliferation (54-56). Activation of  $\text{Ca}^{2+}$  signaling is

regulated by  $\text{Ca}^{2+}$  concentration levels in extracellular and intracellular stores and by the rate of depletion of  $\text{Ca}^{2+}$  concentration (54, 57). The plasma membrane contains ion channels that regulate the supply of calcium ions from the extracellular  $\text{Ca}^{2+}$  stores, and ion channels on the endoplasmic reticulum regulated by cytosolic calcium and  $\text{IP}_3$  concentrations to maintain calcium ion levels in the intracellular stores (58). Ryanodine receptors (RyRs) are activated by cytosolic calcium leading to the release of  $\text{Ca}^{2+}$  from intracellular stores when  $\text{Ca}^{2+}$  concentrations are low in the cytoplasm.

### **Role of intracellular calcium channels in cell death**

Apoptosis of a cell occurs when a cell is unable to carry out proper cellular functions and needs to be removed. Apoptosis is an active and highly regulated process. Apoptosis can become activated by the loss of  $\text{Ca}^{2+}$  homeostatic control by disruption of ion channels (59). The initial concept that  $\text{Ca}^{2+}$  could be a signal for cell death was first put forth by Fleckenstein in 1974, by the proposal that excess  $\text{Ca}^{2+}$  enters myocytes and could cause cardiac pathology (60).  $\text{Ca}^{2+}$  signals the start of apoptosis by DNA fragmentation with the activation of  $\text{Ca}^{2+}$  and  $\text{Mg}^{2+}$  dependent endonucleases. The endoplasmic reticulum (ER) is used for  $\text{Ca}^{2+}$  storage and signaling, and changes in  $\text{Ca}^{2+}$  concentrations by influx or depletion can cause ER stress and signal cell removal by apoptosis (59). Calcium channels become impaired in cancer cells when the channels become compromised and stimulate development of disease. Compromised channels lead to development of tumors, abnormal cell differentiation, migration, and impaired cellular apoptosis (61).

## **Functions of Nampt on intracellular Ca<sup>2+</sup>**

Intracellular Ca<sup>2+</sup> levels are a current focal point for the use of Ca<sup>2+</sup> as a target for pharmacological intervention, since they provide ways to prevent cellular apoptosis. The rationale for this approach is based on the fact that Nampt is a key catalytic enzyme in the production of NAD. NAD can either go towards the creation of NADH or can be recycled back to NAM and ADP-ribose where ADP-ribose will be used for calcium homeostasis (Wang, 2015). Previous studies have shown that the use of a Nampt inhibitor depleted NAD, by noncompetitive inhibition of the enzyme, reducing mitochondrial membrane potential and increasing apoptosis (62, 63). The decrease of NAD levels causes an attenuation of glycolysis decreasing mitochondrial membrane potential and reducing endoplasmic reticulum Ca<sup>2+</sup> levels (64, 65). The induction of apoptosis has not been correlated with the reduction of Ca<sup>2+</sup> levels and the depletion of NAD, but studies suggest that reduced NAD disrupts Ca<sup>2+</sup> levels and NAMPT inhibition induces apoptosis (66).

## **Oxidative stress**

Oxidative stress is caused by the production of reactive oxygen species formed from metabolism of oxygen (67-69). The definition of a reactive oxygen species (ROS) is molecules that come from oxygen and are extremely reactive corresponding to the electrons in their valence shells (70). The most common forms of ROS are superoxide (O<sub>2</sub><sup>-</sup>), hydroxyl radical (OH<sup>-</sup>), and hydrogen peroxide (H<sub>2</sub>O<sub>2</sub>). Generation of ROS can come from other sources as well, including exogenous and mitochondrial production. Exogenous ROS is created from exposure to ultraviolet light, radiation, drugs, toxins, and

chemicals. Mitochondrial ROS is generated through mitochondrial enzymes and the cellular mitochondrial consumption of O<sub>2</sub> (70).

Oxidative stress can damage cells, lipids, proteins, and nucleic acids, but is neutralized by cellular antioxidants (71, 72). There are several ROS, including superoxide, hydroxyl radicals, and hydrogen peroxide that can induce cell death by oxidative stress (73). Oxidative stress is an imbalance between the reactive oxygen species and the cell's ability to detoxify the ROS or repair the damage caused by oxidative stress. Oxidative stress plays a key role in mitochondrial dysfunction which accelerates the aging process and neurodegenerative disorders (74-76). In Alzheimer's disease oxidative stress results in the impairment of energy metabolism where high energy demands are imposed on the cell during oxidative stress and causes an influx of Ca<sup>2+</sup> into the cytoplasm altering intracellular Ca<sup>2+</sup> signaling (77). Preventing oxidative stress-induced changes in Ca<sup>2+</sup> concentrations will cause a slowing of Alzheimer's disease progression by preventing the loss of neuronal cells to apoptosis. Glaucoma patients suffer damage from oxidative stress in the loss of retinal ganglion cells and damage to the trabecular meshwork. Preventing damage from oxidative stress will slow the loss of RGCs and prevent high IOP with survival of TM cells. In AMD oxidative stress causes mitochondrial dysfunction with the loss of mitochondrial DNA, accelerating the aging process and neurodegenerative disorders. If oxidative damage to mitochondrial DNA was reduced DNA repair would allow for restoration of mitochondrial function and normalize energy levels.

Cells that are damaged by disease have shown a higher energy level demand than a non-damaged cell (78). Cell death is diminished when increased levels Nampt are

present to maintain mitochondrial NAD levels (46). The prevention of cell death by increased NAD levels suggests a protective role of Nampt in ischemia, and it may exert protective effects against oxidative stress inducing cell apoptosis. In neuronal cells Nampt provides neuroprotection from oxidative stress, and previous publications showed that oxidative stress in AD results in impaired energy metabolism. Using this novel approach of Nampt being a neuroprotective agent through the production of NAD to prevent apoptosis will allow Nampt's mechanism of action to provide a therapeutic relief for neurodegenerative diseases.

## CHAPTER 2

### MATERIALS AND METHODS

#### **Human rNampt plasmid construction**

Creation of the human rNAMPT.pGEX-6P-1 plasmid construct was created by first using primers designed in house to add on restriction sites BamHI to the sense end and EcoRI to the antisense. A master mix was created using 25  $\mu$ L DreamTaq DNA Polymerase (ThermoFisher Scientific, Waltham, MA), 1  $\mu$ L each of diluted one to ten forward and reverse primers (Integrated DNA Technologies, Skokie, IL), 1  $\mu$ g template DNA, and nuclease-free water up to a total reaction volume of 50  $\mu$ L. This reaction was placed inside PCR grade microtubes and amplification was done using an Applied Biosystems Veriti 96 well Thermo cycle (ThermoFisher Scientific) with protocol: initial denaturation at 95°C for 1 minute, 30 cycles of 95°C for 30 seconds then 60°C for 30 seconds, 72°C for 30 seconds, and final extension at 72°C for 10 minutes with a final hold at 4°C. After completion of PCR 10  $\mu$ L of Nampt PCR product, 1  $\mu$ L of Fast Digest BamHI (ThermoFisher Scientific, Waltham, MA), 1  $\mu$ L Fast Digest EcoRI (ThermoFisher Scientific, Waltham, MA), 4  $\mu$ L of 10X Buffer and nuclease-free water up to a total reaction volume of 40 $\mu$ L. Reactions tubes were placed inside a 37°C water bath and incubated for 20 minutes. Vector pGEX-6P-1 (GE Healthcare Life Sciences, Pittsburg, PA) was digested using the same protocol at the same time as the PCR product. For creation of the plasmid construct BamHI and EcoRI digested Nampt and pGEX-6P-1 recombinant DNA underwent ligation using 1  $\mu$ L T4 DNA ligase (ThermoFisher Scientific, Waltham, MA), 2  $\mu$ L 10X Buffer, 6  $\mu$ L Nampt insert, 2  $\mu$ L pGEX-6P-1, and

nuclease-free water up to a total reaction volume of 20  $\mu$ L. The ligation reaction was incubated at RT for 10 minutes and then transformed into XL1-Blue competent *E. coli* cells (ThermoFisher Scientific, Waltham, MA) and plated on to LB<sup>amp</sup> agar plates and grown at 37°C overnight. Colonies were selected and grown up for DNA collection using Plasmid Kit (BioRad, Hercules, CA) and sent to DNA Analysis Facility (Yale University, Science Hill, CT) for sequencing before use in protein expression and purification and the creation of frozen stock vials.

Creating of site-directed mutagenesis for rNampt was performed by Genscript (Cedarlane, Canada) where His247 was mutated to Ala. A complete sequence of the template with target gene and vector were sent to Genscript, along with mutation specifications and 4  $\mu$ g of template DNA in pGEX-6P-1 vector as starting material. Sequencing was performed by Genscript before the finished product was delivered in lyophilized form. The lyophilized DNA was suspended in PBS before being verified using restriction enzymes BamHI and EcoRI, using the same protocol that was used for rNampt digestion. After verification samples were expressed in *E. coli* cells for protein expression.

### **Expression and purification of human rNampt protein**

Expression of recombinant Nampt was completed by inoculating 50 mL of LB (ThermoFisher Scientific, Waltham, MA) from frozen stock vials and allowing culture to grow over night. For large scale expression 1.5 L of LB was used and inoculated from starter culture. The flask of 1.5L of LB was placed in a shaking incubator at 37°C until an O.D. was reached of 0.6. IPTG was then added at a final concentration of 0.3 mM and

incubated for an additional 3 hours. Bacterial cells were collected via centrifugation and used for bacterial lysate or frozen at -80°C. Collection of rNampt from bacterial lysate was performed using GST lysis buffer, 1µg/mL DNaseI, 100µg/mL lysozyme and placed on a rocker at RT for 30 minutes. Cell lysate was then centrifuged at 20,000xg for 20 minutes and supernatant was filtered using a 0.45 µM syringe filter to remove cell debris.

Purification of rNampt was performed using Profinia Protein Purification System (BioRad, Hercules, CA) with GST column (BioRad, Hercules, CA #732-4622) at 4°C. Samples were released from the GST column by using reduced Glutathione (ThermoFisher Scientific, Waltham, MA 120000010) in the elution buffer and after collection all samples were dialyzed using Slide-A-Lyzer cassettes (ThermoFisher Scientific, Waltham, MA).

### **Validation of expressed rNAMPT via Gel electrophoresis and enzymatic assay**

After collection of dialyzed rNampt protein concentration was determined using BioRad standard protocol for DC Protein Assay Lowry (BioRad #5000111, Hercules, CA) and samples were standardized for Western blot to 20 µg of total protein. PageRuler™ Plus (ThermoFisher Scientific, Waltham, MA) and samples of rNampt and vector only GST were loaded into pre-cast 4-12% Bis-Tris Western blot gels and running buffer NuPAGE® MOPS (ThermoFisher Scientific, Waltham, MA) and ran at 180V for 50 minutes, transferred to nitrocellulose membrane, and blocked using 5% milk with 0.2% Tween 20. Primary antibodies pRb anti-Nampt (Bethyl Montgomery, TX A300-372A) and pGt anti-GST (Abcam Cambridge, MA AB6613) were diluted in 2.5% milk



and allowed to bind to rNampt protein at 4°C overnight. Internal housekeeping proteins and loading controls were targeted using mMs anti-Actin (Millipore Ontario, Canada MAB1501R). Membranes underwent two washes using PBS buffer with 0.2% Tween-20 for 10 minutes before being incubated in anti-mouse, anti-rabbit, or anti-goat IgG horseradish peroxidase (HRP)-linked secondary antibodies. Membranes underwent two washes before the addition of Luminata™ Forte Western HRP substrate (Millipore Ontario, Canada WBLUF0500) for signal development using chemiluminescent. Syngene G:Box and GeneSnap software (Syngene, Frederick, MD) were used to detect band intensity and to create layered images for analysis. Any membranes that had been initially used with other primary antibodies were incubated with membrane stripping buffer to eliminate any detection of previous antibodies. Membranes were sealed within plastic with stripping buffer (20 mM tris-base, 0.2% Triton X-100 (v/v), 6 M guanidine hydrochloride, and 0.7% β-mercaptoethanol, pH 8.0) for 30 minutes at 50°C water bath. Membranes were washed using PBST and then subjected to the above protocol for blocking the membrane and use of a different primary antibody.

Recombinant proteins were tested for enzymatic activity by converting NAM to a NMN derivative from which a detectable fluorescence can be seen with the addition of two steps. Reactions were performed with 5 μL of 0.5 μM NAM and 20 μL of rNampt or rGST mixed with reaction buffer, consisting of 0.4 mM phosphoribosylpyrophosphate (PRPP) (Sigma St. Louis, MO P8296), 12 mM MgCl<sub>2</sub>, 0.02% bovine serum albumin, 2mM dithiothreitol (ThermoFisher Scientific, Waltham, MA 16568-0250), 2 mM ATP (Sigma St. Louis, MO A2383), and 50 mM Tris-HCl (pH 7.5). Reaction buffer and PRPP were frozen at -20°C separately and mixed with 1 mL Buffer and 0.4 μL PRPP,

before performing enzyme assay. The mixture of rNampt, reaction buffer, and NAM were incubated at 37°C for 30 minutes and then heat inactivated at 95°C for 1 minute. Then 10 µL of 2 M KOH and 10 µL of 20% acetophenone (Sigma St. Louis, MO 42163) diluted in DMSO were added to the enzyme mixture and incubate on ice for 2 minutes. The final step was to add 45 µL of 88% Formic acid and incubated for 10 minutes at 37°C. Fluorescence was measured via Synergy H1 plate reader (BioTek, Winooski, VT) excitation 382 nm and emission 445 nm wavelengths. NMN standard curve was performed by using 25 µL NMN standard curve (Sigma St. Louis, MO N3501) and the previous steps used with the enzymatic mixture.

#### **In vitro cell culture of SH-SH5Y cells**

Frozen cell line SH-SY5Y human neuroblastoma cells (ATCC, Manassas, VA) were recovered from liquid nitrogen storage by having the cells thaw on ice, and suspended in 50% Dulbecco's Modified Eagles Medium, 50% Ham-s F12 (Lonza, Walkersville, MD) media containing 10% fetal bovine serum (heat inactivated) (MP Biomedicals, Solon, OH), 100 units/ml penicillin G sodium, and 100µg/ml streptomycin. SH-SY5Y cells were grown in tissue culture flasks (MidSci, St. Louis, MO) and incubated at 37°C and 5% CO<sub>2</sub>. After the cells have reached a confluence of approximately 70-80% by visual microscopy, the media is removed for collection of cells. Five mLs of Trypsin-EDTA (Corning, Manassas, VA) was added to each SH-SY5Y 150mM Flask and allowed to incubate at room temperature for two minutes before the flask was rocked and allowed to rest for one minute. Trypsin cell suspension was then collected and put into a 50mL conical tube for centrifugation at 1000 x g for 2

minutes. The cell pellet was suspended in media and 15  $\mu$ L of cell suspension and 15  $\mu$ L of cell viability dye, trypan blue (EMD Millipore, Billerica, MD) were mixed 1:1 and a Cellometer Auto T4 (Nexcelom Bioscience, Lawrence, MA) was used to calculate cellular concentrations of live cells.

### **In vitro cell culture of ARPE-19 cells**

Frozen cell line ARPE-19 human epithelium cells (ATCC, Manassas, VA) were taken from liquid nitrogen storage and removed from storage media by thawing the cells and suspending them in Dulbecco's Modified Eagles Medium (Lonza, Walkersville, MD) media containing 10% fetal bovine serum (heat inactivated) (MP Biomedicals, Solon, OH), 100 units/ml penicillin G sodium, and 100 $\mu$ g/ml streptomycin. ARPE-19 cells were grown in tissue culture flasks (MidSci, St. Louis, MO) and incubated at 37°C and 5% CO<sub>2</sub>. After the cells have reached a confluence of approximately 70-80% by visual microscopy. The adherent cells were scraped from each flask and the cell suspension was then collected and put into a 50mL conical tube for centrifugation at 1000 x g for 2 minutes. The cell pellet was suspended in media and 15  $\mu$ L of cell suspension and 15  $\mu$ L of cell viability dye trypan blue (EMD Millipore, Billerica, MD) were mixed 1:1 and a Cellometer Auto T4 (Nexcelom Bioscience, Lawrence, MA) was used to calculate cellular concentrations.

### **In vitro cell culture of optic nerve head astrocytes**

Optic nerve head astrocytes (ONHA) cells were collected from three month old male Brown Norway rats from which the optic nerve was dissected for cell collection

(79). ONHA cells were brought up from -80°C storage, thawed on ice, and suspended in Dulbecco's Modified Eagles Medium (Lonza, Walkersville, MD) media containing 10% fetal bovine serum (heat inactivated) (MP Biomedicals, Solon, OH), 100 units/ml penicillin G sodium, and 100µg/ml streptomycin. ONHA cells were grown in tissue culture flasks (MidSci, St. Louis, MO) and incubated at 37°C and 5% CO<sub>2</sub>. After the cells have reached a confluence of approximately 70-80% by visual microscopy the adherent cells were scraped from each flask and the cell suspension was then collected and put into a 50mL conical tube for centrifugation at 1000 x g for 2 minutes. The cell pellet was suspended in media and 15 µL of cell suspension and 15 µL of cell viability dye, trypan blue (EMD Millipore, Billerica, MD) were mixed 1:1 and a Cellometer Auto T4 (Nexcelom Bioscience, Lawrence, MA) was used to calculate cellular concentrations.

### **Cell viability measurement**

Testing of cell viability was done in one of three ways: visual cell counts using a light microscope, Calcein-AM assay or MTT assay. NADPH cellular oxidoreductase enzyme reduces the tetrazolium dye MTT (3-(4,5-Dimethylthiazol-2-yl)-2,5-Diphenyltetrazolium Bromide) (ThermoFisher Scientific, Waltham, MA) to an insoluble form of formazan that is purple in color. The MTT assay was performed similar to previous work with C6 astroglia cells, HT-22 cells, and primary cortical neurons (77, 79, 80) by first creating a working dye solution of 1 mL of 12 mM MTT and 9.5 mL of HBSS. Cell culture media is removed and 100 µL of HBSS buffer or working dye is added to the 96 well plate and incubated for 2 hours at 37°C. Once the dye has been taken up, removal of the working dye solution is done by inverting the plate and adding

100  $\mu$ L of DMSO to each well before mixing the plate on a shaker for 10 minutes to dissolve the cells. Once cells are dissolved an absorbance reading at 570nm can be performed with higher absorbance readings indicating higher cell survival.

To test cellular viability using Calcein-AM assay a stock solution of 4mM Calcein-AM (Life Technologies C3100MP) in DMSO is created and used to make a working solution at 10  $\mu$ M in HBSS After removal of media from 96 well plate 100  $\mu$ L of 4  $\mu$ M Calcein-AM is added per well and incubated for 1 hour in a 37°C oven. Removal of the Calcein solution is done by inversion and 100  $\mu$ L of clean HBSS is added to each well before reading the fluorescence at 485 excitation and 525 emission. Higher cell survival would be seen with wells emitting higher fluorescence due to esterase activity cleaving the Calcein-AM.

### **Optimization of oxidative insult**

Testing of the optimal concentration of *tert*-butyl hydroperoxide (tBHP, Sigma 458139) was performed by plating 10, 000 cells per well of SH-SY5Y, 7,500 cells per well of ARPE-19, or 5,000 cells per well of ONHA on day one. On day two tBHP concentrations were prepared in cell culture media and 100  $\mu$ L of tBHP media was added to treatment wells and incubated overnight. SH-SY5Y concentrations ranged from 0 to 200  $\mu$ M, ARPE-19 from 0-300  $\mu$ M, and ONHA from 0-300  $\mu$ M. Cell viability was tested on day three by using the MTT viability assay. In order to assess the impact of tBHP treatment a 70% kill rate was required in order to measure any effects that are provided by the addition of rNAMPT.

### **Cellular protection assay and treatment with rNAMPT**

Plates were divided so that each treatment would have a total of 8 wells allowing for 8 replicates and each plate was a different passage for each cell line. Protection assays for SH-SY5Y, ARPE-19 and ONHA cells were each plated on day one at the concentrations used for the tBHP optimization tests and placed in 37°C incubator with 5% CO<sub>2</sub>. On day two pre-treatment of 1 μM rNampt in fresh media was added to each well for a total of 200 μL and placed back into the incubator for 4 hours. After the pre-treatment tBHP was diluted in media and placed in the 96 well plate for a total 300 μL media and the optimized tBHP concentration and incubated overnight for 14-16 hours. Visual cell counts were performed following overnight incubation of tBHP. Images were taken of three different fields of view per well and living cells were counted.

### **siRNA knockdown of Nampt**

Optimization of transfection using Lonza 4 D-Nucleofector (Lonza, Switzerland) was used with buffer kit P3 for primary cell line optimization. Cell lines ARPE-19 and ONHA were collected and cell counted for 100,000 cells per reaction. Each reaction was a mixture of Nucleofector<sup>tm</sup> P3 solution, Supplement, and 0.4 μg pmaxGFP<sup>tm</sup> Vector were pipetted into 20 μL Nucleocuvette® strip. Once transfection was complete cells were allowed to rest at RT for 10 minutes before adding 80 μL fresh media, then all 100 μL were transferred to a 12 well dish and placed in an incubator overnight. The following day cells were imaged using white light to look at cell survival and visually counted; along with GFP excitation to look for percent transfection of each protocol.

Transfection of ARPE-19 was performed using Lonza P3 buffer kit and optimized protocol DS 109 (81). Lonza cuvette protocol was used with 500,000 cells per reaction, 82  $\mu$ L P3 solution, 18  $\mu$ L supernatant, and 200 nM of each Nampt siRNA. The siRNA Nampt (Origene SR306835) silence the respective gene and were designated NAMPT-A, NAMPT-B, and NAMPT-C (Table 1) and transfection concentration of 200 nM were based on recommendations from Origene. Once transfection was complete cells were allowed to rest at RT for 10 minutes before adding 500  $\mu$ L fresh media, then all 600  $\mu$ L were transferred to a T75 cell culture flask and incubated overnight at 37°C and 5% CO<sub>2</sub>. After 24 hours of incubation and cell growth, cells were scraped from the bottom of the flask and protein was extracted. Cell lysate was collected using 100  $\mu$ L of Cytobuster (Novagen 71009) and inhibitor (Thermo Scientific 78430) and re-suspended by pipetting. The cell suspension was then vortexed for one minute before being pulled up via insulin syringe (BD 324910) before being centrifuged at 16,300 x g for 5 minutes. Supernatant was collected and protein concentration was calculated by Lowry assay and samples were loaded into precast Western blot gels. Primary antibody pRb anti-Nampt and loading control mMs anti-Actin. Transfection of cell line ONHA was performed under the same procedure but the Lonza transfection protocol was changed to EL 110 (81).

## CHAPTER 3

### RESULTS

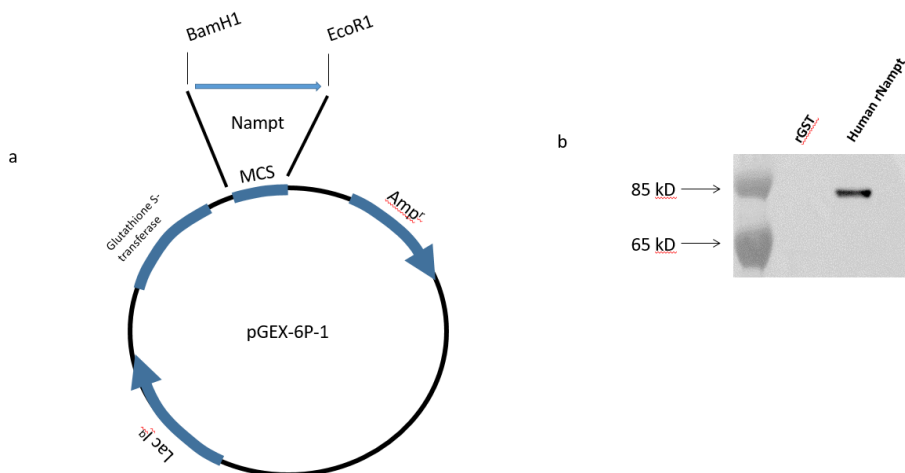
#### **Human recombinant Nampt plasmid**

To assess the neuroprotective properties of Nampt, recombinant Nampt (rNampt) protein was expressed in *E. coli* cells and purified. Figure 1 A shows the Nampt expression construct used to generate recombinant GST tagged Nampt. The coding sequence of Nampt was cloned into the pGEX-6P-1 vector using the restriction sites of BamH1 and EcoR1.

The identity of purified rNampt was verified by Western blotting using the affinity purified polyclonal human pRb anti-Nampt antibody. Nampt appeared as a single band with the expected molecular weight of 79 kDa for GST (27kDa) tagged Nampt (52kDa) (Fig. 1B).

Figure 1. Expression of human recombinant Nampt (rNampt) protein. (A) Full restriction map and vector for human rNampt. The coding sequence of Nampt was cloned into the multiple cloning site (MCS) of the pGEX-6p-1 protein expression vector using the restriction sites BamH1 and EcoR1. (B) Western Blot comparison of bacterial expressed recombinant proteins rGST (negative control) and human rNampt using the affinity purified polyclonal pRb anti-Nampt antibody. Nampt was detected as a single band of approximately 79kDa, which was expected for GST tagged Nampt.



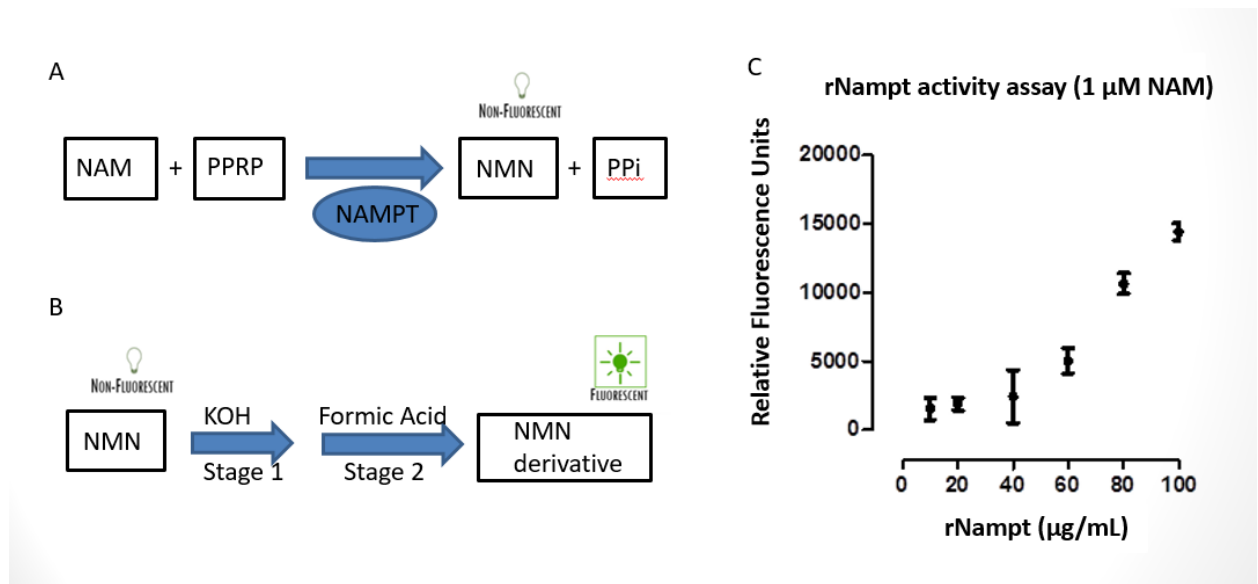


### Enzymatic activity profile of rNampt

Nampt is the regulator of the NAD<sup>+</sup> pool. The synthesis of NAD<sup>+</sup> from NAM involves the conversion of NAM to NMN, which is catalyzed by NAMPT (Fig 2A). rNampt was tested for enzymatic activity using the plate reader assay. rNampt showed increasing enzymatic activity as measured by the ability of Nampt to catalyze the reaction where NAM is converted to NMN derivative and the fluorescence of NMN is measured (Fig 2B). rNampt showed a dose dependent increase in enzymatic activity using 1  $\mu$ M NAM substrate. (Fig. 2C).

Figure 2. Conversion of Nicotinamide to fluorescent Nicotinamide mononucleotide derivative: (A) Nampt enzyme activity reaction. Nampt catalyzes the reaction where the substrates nicotinamide (NAM) and 5-phosphoribosyl-1-pyrophosphate (PRPP) is converted to the products nicotinamide mononucleotide (NMN) and pyrophosphate (PPi). (B) Detection reaction. Relative Nampt activity can be determined by quantifying the

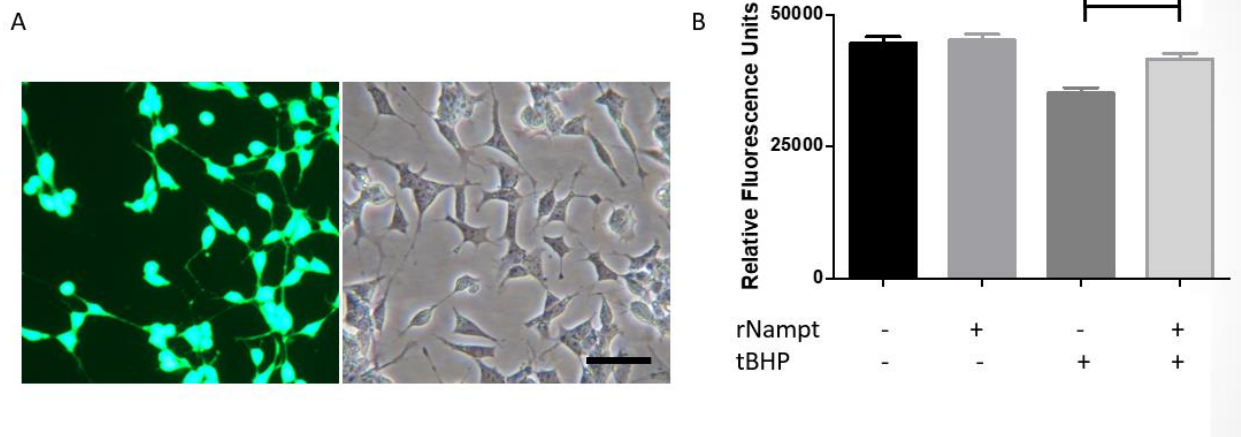
NMN product. To convert N-alkylpyridinium compounds into fluorescent derivatives, reactions involving ketones followed by heating in excess acid is performed. NAM was converted to NMN and the NMN product was converted to a fluorescent derivative through reacting with acetophenone/KOH followed by formic acid (Fig. 2B). (C) Relative Nampt activity was determined by measuring the fluorescence derivative of NMN. Increasing concentrations of rNampt was used to measure Nampt enzyme activity along with sufficient amount of NAM. Nampt activity showed a concentration dependent increase.



### **rNampt is neuroprotective against oxidative stress in SH-SY5Y cells**

To address if rNampt could provide neuroprotection the human neuroblastoma cell line SH-SY5Y was used. It was chosen based on its sensitivity to the oxidative stress exogenous inducer, *tert*-butyl hydroperoxide (tBHP) and work done by our lab and others demonstrating it as a good model for neurodegenerative research. SH-SY5Y cells were pre-treated with 100 nM rNampt for 4 hours followed by the addition of the neurodegenerative insult, the ROS agent, tBHP, at 25  $\mu$ M. The calcein-AM assay was used to determine cell viability. Calcein AM is a membrane permeable green fluorescent marker and is introduced into cells by incubation. Once inside the cells, calcein AM, a non-fluorescent calcein ester is cleaved by intracellular esterase and the non-fluorescent compound (Calcein-AM) is converted to a green-fluorescent compound (Calcein). The green fluorescent calcein is retained in the cytoplasm in live cells which is measured using 485 excitation wavelength and 530 nm emission wavelength. The fluorescent signal generated is proportional to the number of living cells in the sample. SH-SY5Y pre-treated with rNampt had significant cell viability compared to cells treated with oxidative stress alone (Fig. 3A-B).

Fig.3. Neuroprotective properties of rNampt in the neuronal SH-SY5Y cells. (A) Microphotographs of SH-SY5Y cells treated with Calcein-AM and DIC mages. (B) Cell viability was measured using Calcein-AM. Cells that remain intact will take up Calcein-AM and fluoresce green. Cells treated with tBHP alone showed decreased viability while cells pretreated with rNampt 4 hours before tBHP treatment showed significant cell viability compared to tBHP treated cells alone.

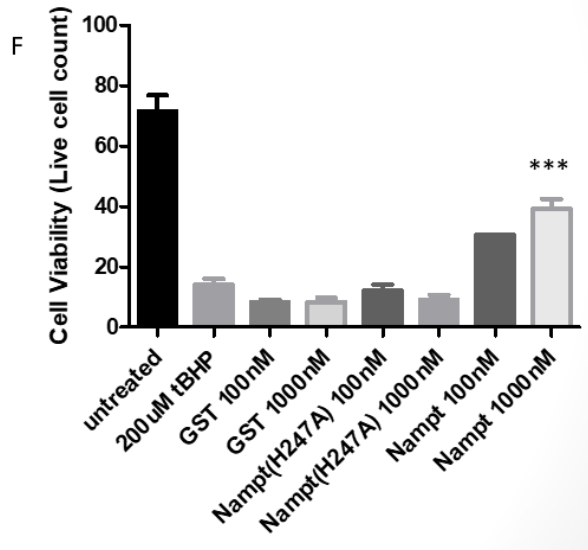
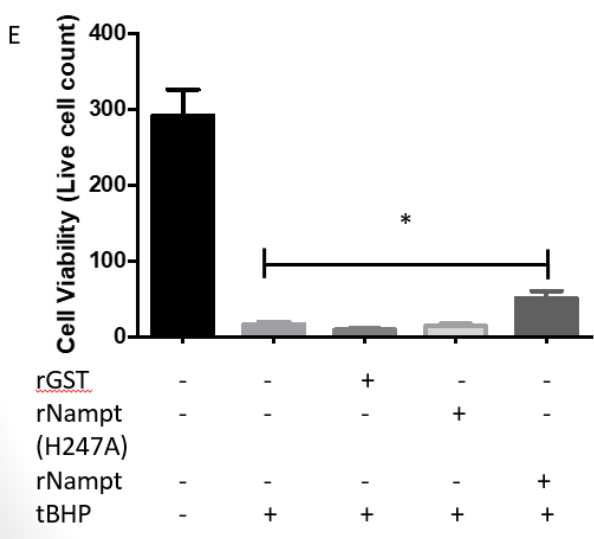
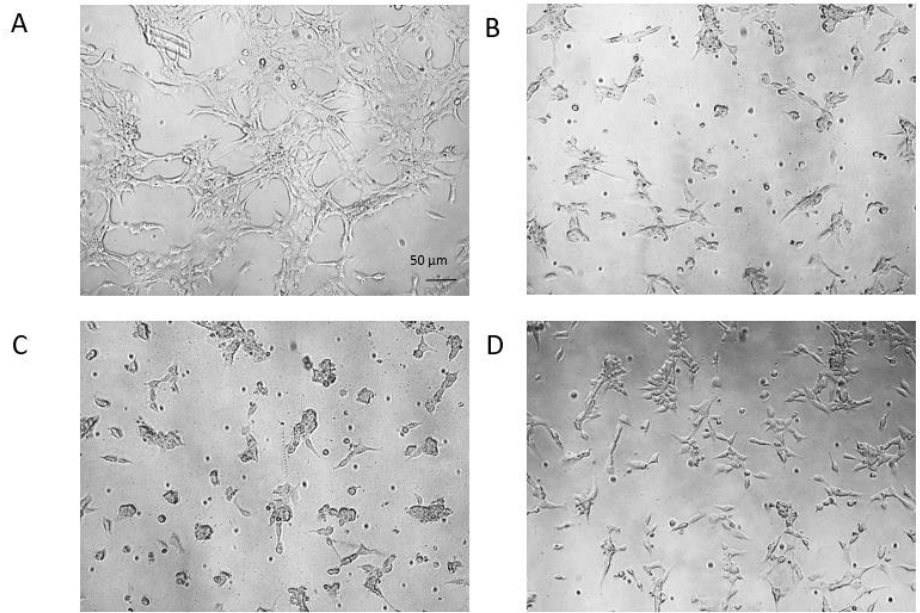


### Neuroprotective properties of rNampt in ARPE-19 cells during oxidative stress

Using SH-SY5Y provided useful information in testing the ability of rNampt to provide neuroprotection in a transformed cell line modeling neuronal cells. As neurodegeneration is often accompanied by degeneration of cell types supporting the role of neurons, a different cell line was tested, retinal pigmented epithelium (ARPE-19). The human ARPE-19 cells is derived from the eye and has been used to model age related macular degeneration (AMD), which is a neurodegenerative retinal disease that is similar to AD in clinical and pathological functions (82). We tested whether rNampt would provide the same protective effects as observed with the SH-SY5Y cell line. ARPE-19 cells were pretreated with either control rGST, the catalytically inactive form of Nampt (rNampt (H247A)), or active rNampt for 4 hours followed by treatment with the tBHP ROS agent to induce oxidative stress. To determine viability, ARPE-19 cells were counted. Cells pretreated with 100nm of rNampt showed protective effects compared to negative controls GST and the catalytic inactive form of Nampt (rNampt (H247A)) (Fig.

4E). In addition, increasing the concentration of rNampt to 1000 nm increased its protective effects (Fig. 4F). When visually looking at the cells, cells treated with rNampt (Fig. 4D) were healthier in appearance compared to the catalytic inactive form of Nampt (H247A) (Fig. 4C). This suggests that Nampt must be active to have protective properties. In order to determine cell viability in ARPE-19 cells we had to manually count viable cells based on morphology. When cell viability was measured with MTT or Calcein-AM both alive and dead cells emitted fluorescence due to the long half-life of the esterases that cleave the substrate. Due to esterase activity MTT and Calcein-AM cell viability assays could not be used with cells ARPE-19 but were successfully tested with SH-SY5Y cells. This required us to manually count the viable cells based on morphology.

Fig.4. Neuroprotective properties of rNampt in ARPE-19 cells undergoing oxidative stress. Microphotographs of ARPE-19 cells that were either (A) untreated, (B) tBHP treated, (C) pretreated with inactive rNampt or (D) active rNampt followed by tBHP treatment. Cells that were pretreated with active rNampt were protected against oxidative stress, while cells treated with the inactive rNampt or left untreated were not. (E) ARPE-19 cell viability was manually determined. Cells pretreated with 100 nm rNampt showed significant protection compared to cells pretreated with rGST or inactive rNampt (H247A) followed by tBHP addition. (F) The protective properties of rNampt was increased when more rNampt (1000 nm) was used.



### Optimization of Nampt knockdown using siRNA in ARPE-19 cells

We wanted to determine what would happen if we removed endogenous Nampt using siRNA where the protein levels would be reduced and Nampt activity would be reduced. To do this we used siRNA to target the knockdown of Nampt (Table 1). The

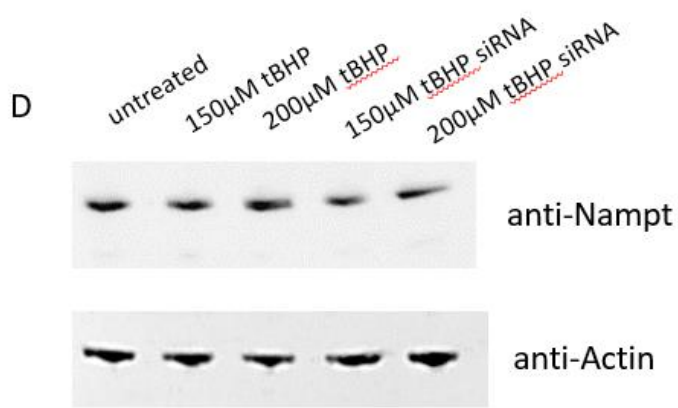
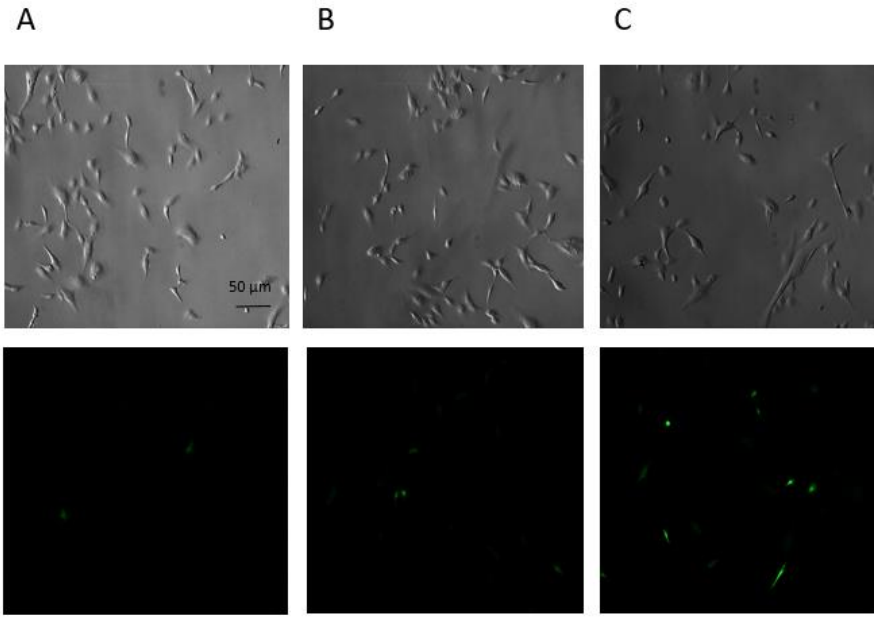
transfection efficiency was assessed for ARPE-19 cells under 8 different electroporation pulse codes using pmaxGFP. pmaxGFP is a plasmid that expresses GFP and is used to determine how many cells received the plasmid based on GFP fluorescence. To assess transfection of ARPE-19 cells were treated under optimization suggestions provided by Lonza 4D-Nucleofector kit. Eight different conditions, which vary on how each well is pulsed with electrical current, were tested in small reaction under the 20  $\mu$ L strip protocol alongside fluorescence insert DNA pmaxGFP. After transfection, cells were allowed to recover and grow for 24 hours before transfection efficiency rates were determined by DIC and fluorescence microscopy. Lonza pulse codes CM102, DC100, and ED100 had low cell survival and poor efficiency lower than 20%. Pulse codes EA104, EL110, and CM113 had 20-40% cell survival and an efficiency of 20% and the highest efficiency of 40% was seen in pulse code DS109. (Fig. 5A-C). After optimization ARPE-19 cells were transfected with siRNA ABC and allowed to recover over a 24 hour period before being treated with 150  $\mu$ M and 200  $\mu$ M tBHP. Cell lysate was collected and Western blots were ran with 20  $\mu$ g total protein and pRb anti-Nampt. Total Nampt protein was seen at a reduced level in cells that were transfected with siRNA when tested with pRb anti-Nampt (Fig. 5D). At both 150  $\mu$ M and 200  $\mu$ M siRNA quantitative results normalized to Actin show that the overall level of expressed endogenous Nampt drops 90% (Fig 5E).

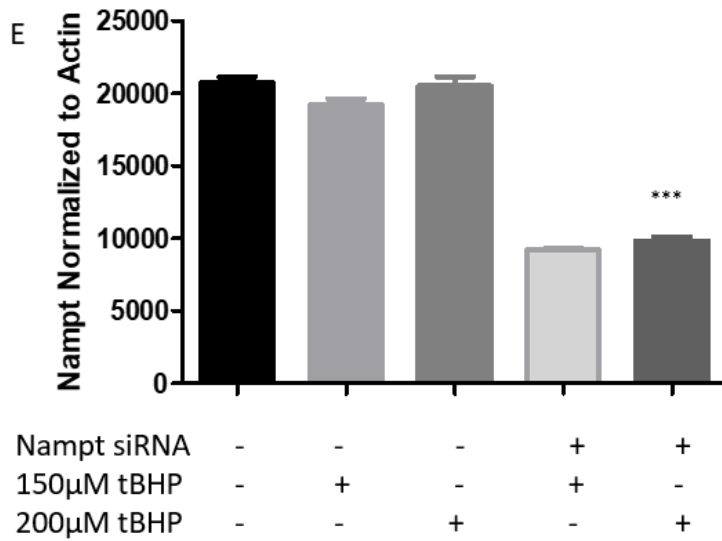
Table 1. Each individual siRNA and its corresponding targeting sequence

siRNA	NAMPT Sequence
NAMPT-A	AGAAUCUUAAGUUGGCUAAAUUCAA
NAMPT-B	GACAUACCCUAUAGAAUUACUAACC
NAMPT-C	ACAUGUAGUGAGAACAAUAAGCAT

Fig.5. Optimization of Nampt knockdown using siRNA in ARPE-19 cells. (A) Electroporation pulse code CL100 showed 20% cell survival and 2% pmaxGFP expression. (B) Electroporation pulse code CM113 showed 20% cell survival and 20% pmaxGFP expression. (C) Electroporation pulse code DS109 showed 20% cell survival and 40% pmaxGFP expression. All pulse codes resulted in neuronal loss when compared to non-transfected ARPE-19 cells (D) Western blot of cell lysate collected from Nampt knocked down with 200 $\mu$ M siRNA comparing treatment with tBHP. (E) Quantitative results of normalized density (Nampt) when compared to actin from Western blot to determine overall knockdown expression of endogenous Nampt.





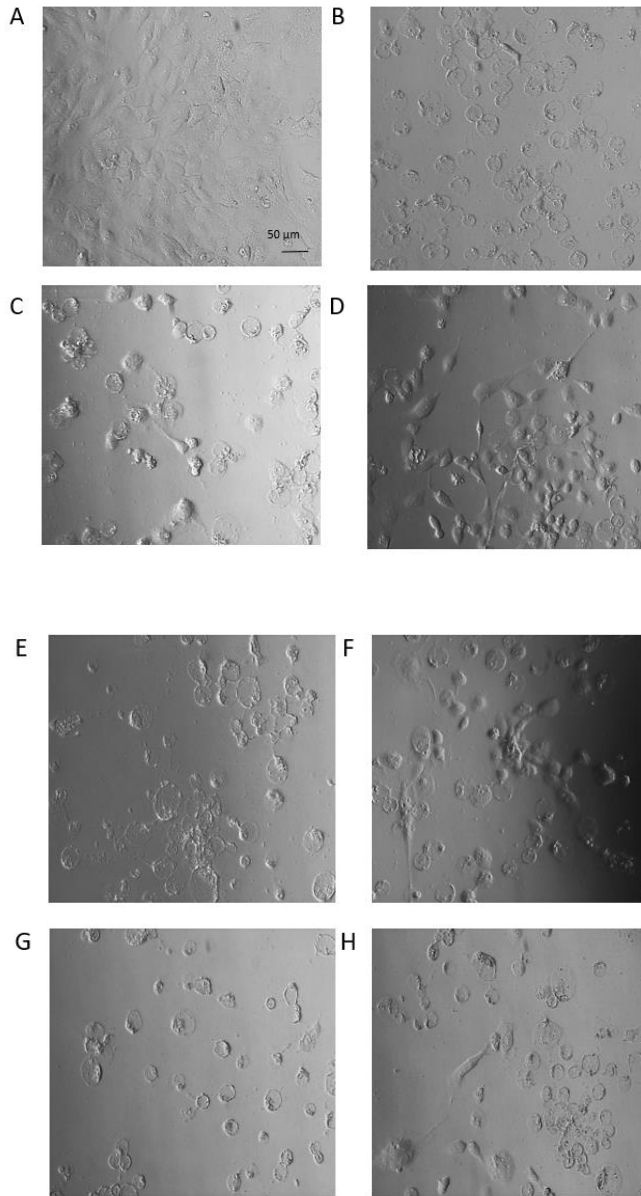


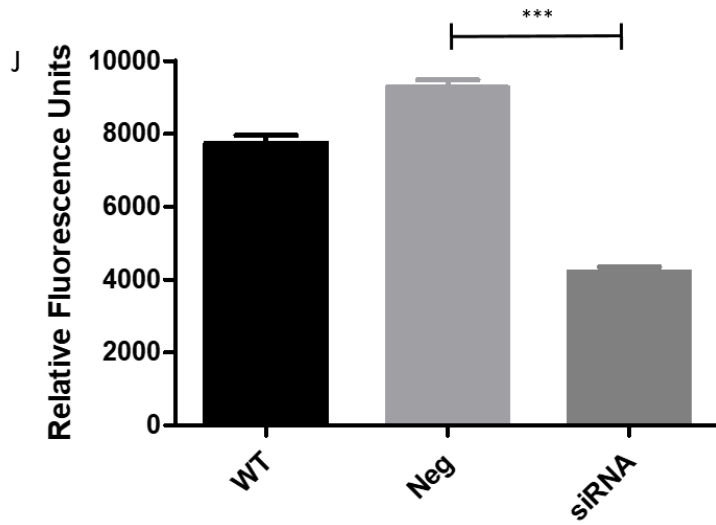
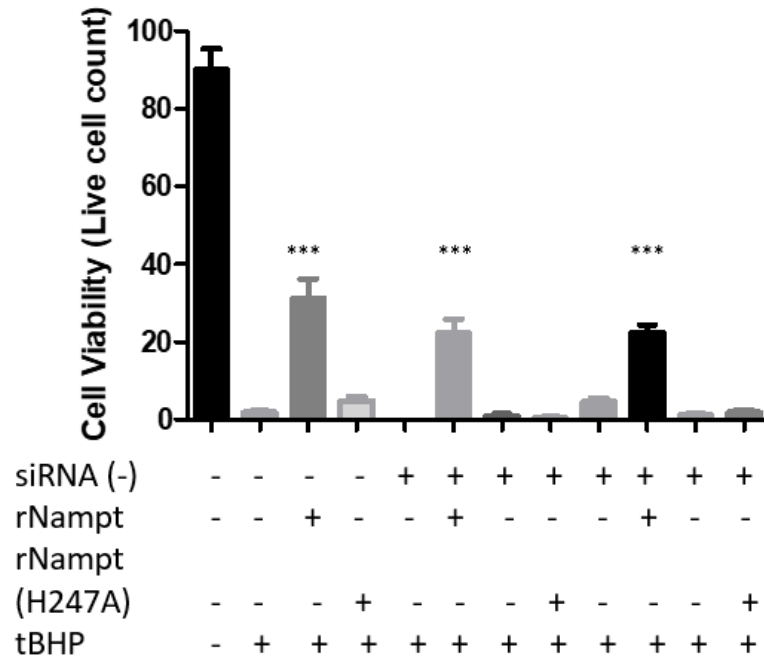
**Knockdown of Nampt by RNAi makes ARPE-19 cells more susceptible to oxidative stress** To determine whether removal of endogenous Nampt from ARPE-19 cells would be effected from oxidative stress siRNA to knockdown Nampt was performed in order to remove Nampt protein. ARPE-19 cells were transfected with Nampt siRNA ABC and allowed to recover and grow for 24 hours. ARPE-19 cells were then treated with tBHP to induce oxidative stress. Knockdown of Nampt in ARPE-19 cells led to faster cell death and more cell death overall after oxidative stress compared to cells that were treated with tBHP with no siRNA or ARPE-19 cells transfected with negative control siRNA. To determine if rNampt could rescue the RNAi we pretreated cells 1 µM rNampt and 4 hours later cells were treated with tBHP using the same protocol that was used to test cellular viability. ARPE-19 cells showed similar results as those of the cellular viability, tested before, where cells treated with catalytic inactive rNampt(H247A) had 0-1% cell survival and cells treated with rNampt had a significant recovery (Fig. 6 A-D). The cells that underwent siRNA ABC transfection show similar results with inactive rNampt or no

Nampt present where there was no significant difference when compared to tBHP treatment (Fig. 6E, G, H). While the cells that were pre-treated with rNampt showed significantly reduced amount of cell death after tBHP treatment (Fig. 6F). Significant cell survival was seen in cells that were pretreated with rNampt prior to tBHP treatment. This includes ARPE-19 cells pretreated with rNampt, ARPE-19 cells transfected with Nampt siRNA followed by pretreatment with rNampt or cells transfected with the negative control siRNA followed by pretreatment with rNampt (Fig. 6I). While all other cells showed no significant change from tBHP treatment indicating that the addition of extracellular rNampt provides protective effects against ROS. Conversion of NAM to NMN for the production of NAD was also measured after for knockdown of endogenous Nampt in ARPE-19 cells. Cell lysates from WT, negative control siRNA (-) and Nampt knockdown were tested for Nampt activity. ARPE-19 cell lysates where Nampt is knockdown showed a significant reduction of relative fluorescence, which indicates reduction in Nampt activity (Fig. 6J).

Fig.6. Knockdown of Nampt in ARPE-19 cells using siRNA: Microphotographs of ARPE-19 cells that were (A) Untreated, (B) treated with 200 $\mu$ M tBHP, (C) pretreated rNampt(H247A) or (D) WT rNampt followed by tBHP treatment, (E) transfected with Nampt siRNA without pretreatment with rNampt or (F) with rNampt followed by tBHP treatment, (G) transfected without siRNA followed by treatment without rNampt (H247A) or (H) with rNampt (H247A) followed by tBHP treatment. (I) ARPE-19 cells were manually counted after siRNA knockdown and pre-treatment with Nampt followed

by tBHP treatment. (J) Nampt Enzymatic Activity of ARPE-19 cell lysate after siRNA knockdown of Nampt.

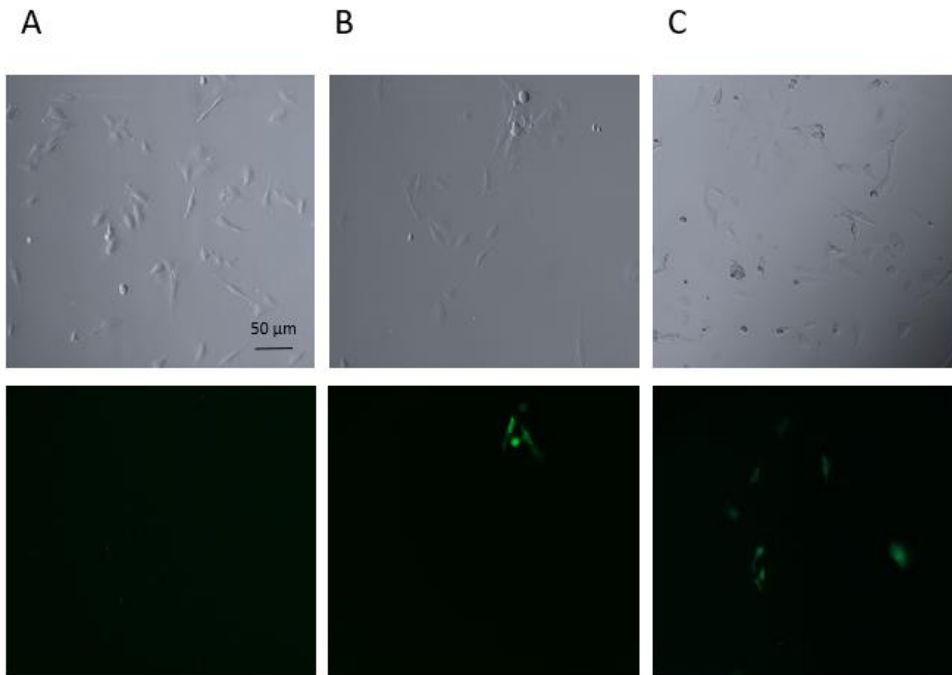


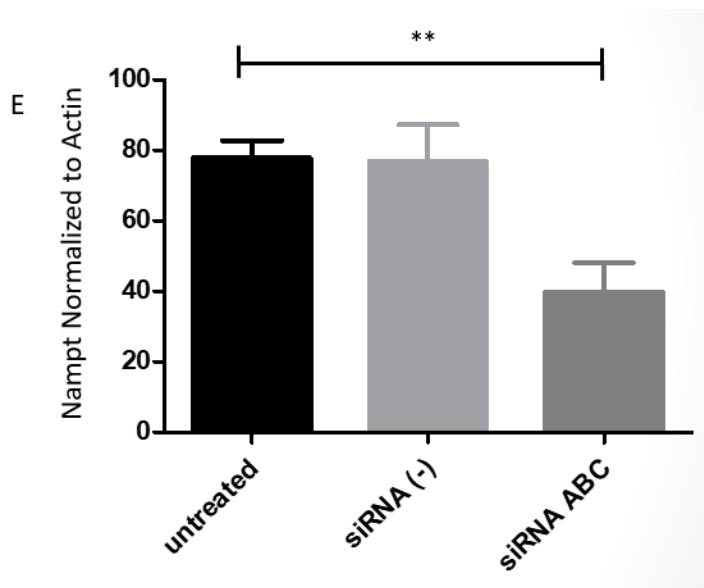
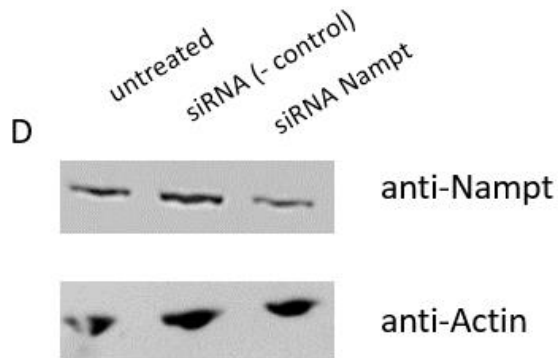


## **Optimization of Nampt knockdown using siRNA in ONHA cells**

A characteristic feature of glaucoma is progressive loss of retinal ganglion cells. Evidence points to the optic nerve head as the point of attack to ganglion cell axons in glaucoma. A meshwork of astrocytes forms the direct environment of the axons. Following an insult to the optic nerve, the astrocytes in the optic nerve head become reactive. This led us into using the optic nerve head astrocytes (ONHA) as a model for glaucoma and to test whether Nampt could be used as a possible therapy. First, we optimized the transfection efficiency of ONHA cells and used pmaxGFP as our control. Optimization of the transfections of ONHA cells was performed by using the same 8 different electroporation pulse codes that were used in ARPE-19 cells and efficiency rates were determined by DIC and fluorescence microscopy. pmaxGFP was used because we can visually see GFP positive cells which indicates that the transfection of the pmaxGFP plasmid worked. Lonza pulse codes CM102, and DC100 had almost no cell survival and expression of pmaxGFP was seen to be 0%. Pulse codes EA104, CM113, and DS109 had 20% cell survival and an efficiency of 10%. The highest cell survival and expression efficiency of 25% was seen in pulse code EL110 (Fig. 7A-C) Using optimized electroporation pulse code EL110 ONHA cells were transfected with Nampt siRNA ABC and allowed to recover for 24 hours. Cells were collected and cell lysate was ran on Western blots with 20  $\mu$ g of total proteins and pRB anti-Nampt. Total Nampt protein was seen at a reduced level in cells that were transfected with siRNA when tested with pRb anti-Nampt (Fig. 7D). At 200  $\mu$ M siRNA ABC quantitative results from the Western blot normalized to Actin show an overall level of expressed endogenous Nampt drops 50% (Fig. 7E).

Fig.7. Optimization of Nampt knockdown using siRNA in ONHA cells (A) Electroporation pulse code CL100 showed 20% cell survival and 0% pmaxGFP expression (B) Electroporation pulse code DS109 showed 10% cell survival and 10% pmaxGFP expression (C) ) Electroporation pulse code EL110 showed 20% cell survival and 25% pmaxGFP expression. All pulse codes resulted in cellular loss when compared to non-transfected ONHA cells (D) Western blot of cell lysate collected from Nampt knocked down with 200 $\mu$ M siRNA comparing Untreated ONHA, siRNA (-) control transfection and siRNA ABC transfection (E) Quantitative results of normalized Density (Nampt) when comparing actin from Western blot to determine overall knockdown expression of endogenous Nampt.





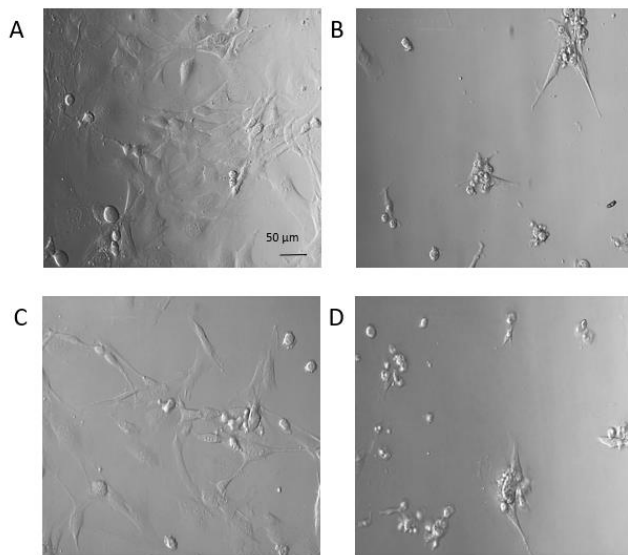
### **Knockdown of Nampt in ONHA cells makes them more sensitive to oxidative stress**

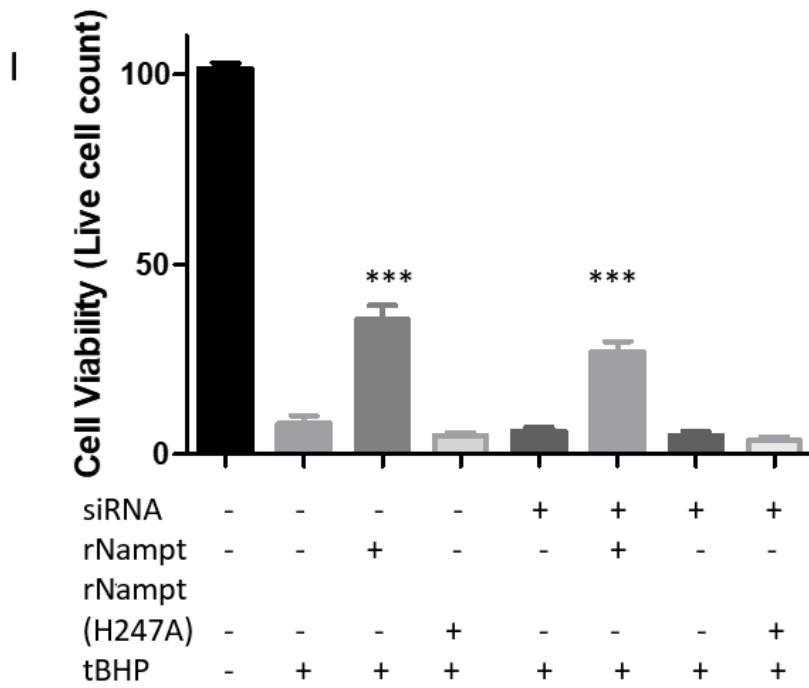
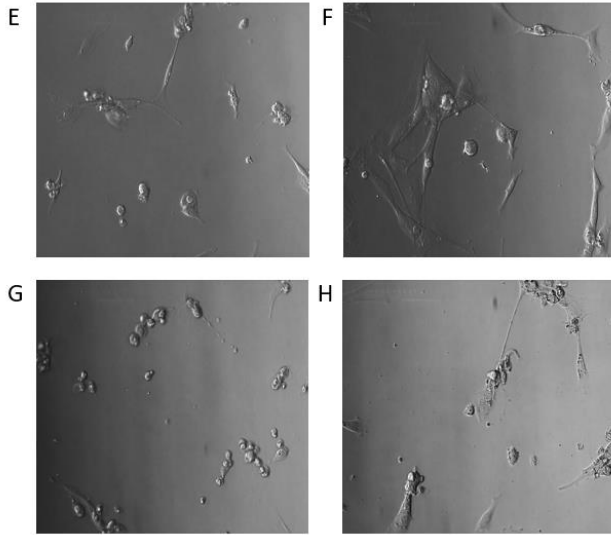
To determine whether Nampt was necessary for ONHA function, we used siRNA to knockdown endogenous Nampt. ONHA cells were transfected with siRNA for Nampt and 24 hours later cells were treated with tBHP to induce oxidative stress. ONHA cells that had reduced Nampt reacted to oxidative stress in the same manner as un-transfected cells treated with tBHP. In both instances ONHA cells died due to the oxidative damage.

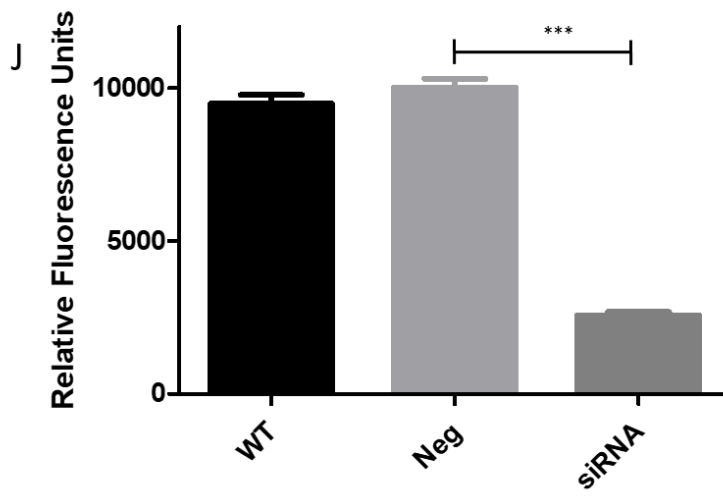


Next, we wanted to determine whether rNampt could rescue the siRNA and protect cells against oxidative stress. To determine if rNampt could rescue the RNAi we pretreated cells with 1  $\mu$ M rNampt and 4 hours later cells were treated with tBHP using the same protocol that was used to test cellular viability. ONHA cells showed similar results as those of the cellular viability, tested before, where cells treated with catalytic inactive rNampt(H247A) had 0-1% cell survival and cells treated with rNampt had a significant recovery (Fig. 8 A-D). The cells that underwent siRNA ABC transfection show similar results with inactive rNampt or no Nampt present where there was no significant difference when compared to tBHP treatment (Fig. 8E, G, H). While the cells that were pre-treated with rNampt showed significantly reduced amount of cell death after tBHP treatment (Fig. 8F). Significant cell survival was seen in cells that were pretreated with rNampt prior to tBHP treatment. This includes ONHA cells pretreated with rNampt, ONHA cells transfected with Nampt siRNA followed by pretreatment with rNampt or cells transfected with the negative control siRNA followed by pretreatment with rNampt (Fig. 8I). While all other cells showed no significant change from tBHP treatment indicating that the addition of extracellular rNampt provides protective effects against ROS. Conversion of NAM to NMN for the production of NAD was also measured after for knockdown of endogenous Nampt in ONHA cells. Cell lysates from WT, negative control siRNA (-) and Nampt knockdown were tested for Nampt activity. ONHA cell lysates where Nampt is knockdown showed a significant reduction of relative fluorescence, which indicates reduction in Nampt activity (Fig. 8J).

Fig.8. Knockdown of Nampt in ONHA cells using siRNA: Microphotographs of ONHA cells that were (A) Untreated, (B) treated with 150 $\mu$ M tBHP, (C) pretreated WT rNampt or (D) rNampt (H247A) followed by tBHP treatment, (E) transfected with Nampt siRNA without pretreatment with rNampt or (F) with rNampt followed by tBHP treatment, (G) transfected without siRNA followed by treatment without rNampt (H247A) or (H) with rNampt (H247A) followed by tBHP treatment. (I) ONHA cells were manually counted after siRNA knockdown and pre-treatment with Nampt followed by tBHP treatment. (J) Nampt Enzymatic Activity of ONHA cell lysate after siRNA knockdown of Nampt.







## CHAPTER 4

### DISCUSSION

Major neurodegenerative diseases that cause debilitating conditions in today's society are linked to cellular damage by oxidative stress (8, 31). Finding new therapies that can be used as a treatment for patients when no other options are available is a pressing concern. The novel mechanisms action of extracellular human recombinant Nampt was tested for potential neuroprotective effects in Alzheimer's disease, age-related macular degeneration, and Glaucoma.

NAD<sup>+</sup> has numerous functions in diverse biological processes, including metabolism, circadian rhythms, aging, and neurodegeneration. In the present study, we showed that human recombinant *NAMPT*, the rate-limiting enzyme in mammalian NAD<sup>+</sup> biosynthesis, played a part in cell survival and death. *NAMPT* acted as a neuroprotective agent against oxidative stress induced by tBHP in a variety of cell lines and knockdown of *NAMPT* by siRNA made the cells more sensitive to oxidative stress induced cell death. Growing evidence shows that *NAMPT* expressed in neurons has neuroprotective effects during ischemic brain injury and that knocking out *NAMPT* in neurons or inhibiting *NAMPT* injured neurons (83-85). In addition, *NAMPT*-mediated NAD<sup>+</sup> biosynthesis is indispensable for photoreceptor survival and vision. The disruption of *NAMPT*-mediated NAD<sup>+</sup> biosynthesis in rod and cone photoreceptors leads to photoreceptor death, retinal degeneration, and blindness (86).

The use of NAD as a nutritional/therapeutic supplement could provide a way to boost NAD<sup>+</sup> biosynthesis in a person suffering from many forms of diseases. The use of

vitamin B3 has been given to people with B3 deficiency where they are unable to obtain it from their food and stimulates NAD<sup>+</sup> biosynthesis (87). Retinal degenerative diseases require high energy levels and depletion of NAD has been seen in the disease. The use of precursors for activation of sirtuins for NAD<sup>+</sup> biosynthesis reduces photoreceptor cell death (88). Nicotinamide riboside has been used as a way to rescue mitochondrial defects and neuronal loss in fly models of Parkinson's disease. Neurons undergo stress response and loss of mitochondrial dysfunction leading to loss of NAD<sup>+</sup> levels. The use of nicotinamide riboside prevented the neuronal loss in fly models GBA-PD (89)

**Human recombinant *NAMPT* protein provides neurodegenerative protection against *tert-butyl hydroperoxide* mediated cell death**

Testing the hypothesis that human rNampt exerts protective effects against oxidative stress in established *in vitro* models of neurodegeneration and cellular degeneration was performed on neuroblastoma cell line SH-SY5Y using ROS simulant tBHP. Initial tBHP treatment with SH-SY5Y cells showed that treatment with tBHP induced oxidative stress and cells underwent apoptosis. SH-SY5Y cells that had undergone a pre-treatment using rNampt, delivered to the cells via fresh media, before the addition of tBHP showed an increase in cell survival, with no observed toxic effects of rNampt (Fig. 1B). The Calcein-AM cell viability assay showed that higher levels of esterase activity were present in untreated cells and those cells that were treated with rNampt, producing higher relative fluorescence values than cells treated with tBHP alone. After successful testing with rNampt in SY-SY5Y cell line showing neuroprotective effects, the cell line ARPE-19 was chosen to be an *in vitro* model for AMD. Protection

of ARPE-19 cells from oxidative stress using rNampt would show that apoptosis could be prevented with NAD<sup>+</sup> production for AMD damaged cells. As seen before when cells are treated with tBHP cell viability decreased when compared to untreated due to oxidative stress and apoptosis. Cells showed similar affects when pre-treated with recombinant proteins that provide no neuronal protection, rpGEX and rNampt(H247A); cells were shown to enter apoptosis at the same rate of the cells that were treated with tBHP only. In the inactive mutant rNampt(H247A) of rNampt the removal of the active site was achieved without any change in the structure or size of the NAMPT protein. We believe the NAMPT structure was not changed and the addition of the inactive rNampt(H247A) acted as a dominant negative for endogenous Nampt. Any effects in the form of cytokine or growth hormone did not play any part in neurodegenerative protection, but protective effects came from the ability to convert NAM to NMN for production of NAD<sup>+</sup>. The addition of rNampt again showed significant improvement in cell viability (Fig. 2E) and matched results seen with the SY-SY5Y cell line. A third cell type, Optic Nerve Head Astrocyte was tested in order to see if rNampt could provide protective effects for glaucoma. When the cells are treated with tBHP cell viability decreases and apoptosis is observed (Fig. 9I). Higher concentrations of rNampt allowed for a significant improvement with a protective effect (Fig. 2F) and offer evidence that exogenously applied rNampt is generating more NMN for production of NAD and is providing is playing a role in neuroprotection with the addition of more NADH production. The treatment of rNampt to all cell lines showed improvement in cell survival, and neuroprotection from oxidative stress.

With the knockdown of Nampt via siRNA transfection in ARPE-19 cells and ONHAs loss of cellular viability with the loss of NAD production during oxidative stress was observed. Removal of Nampt resulted in complete cell death but if extracellular rNampt was present production of NAD provided protective effects for the cells and activation of cellular apoptosis was diminished (Fig. 7I). Unlike the situation in cardiac myocytes, in which that when Nampt knockdown leads to loss of all cells due to apoptosis with no treatment (90). Neuronal cells are only sensitive to knock down of Nampt indicating possible check points to prevent complete cell loss as seen with the use of Nampt knockdown using siRNA.

### **Experimental approach and technical limitations impacting Nampt-mediated neuroprotection**

To measure neuronal protection by NAMPT, a human neuroblastoma cell line was pre-treated with human rNampt and oxidative stress was simulated via ROS. The goal for this experiment was to see if extracellular rNampt could provide this neuronal protection via the production of NAD<sup>+</sup> and counter the increased energy demands of damaged cells. Using one cell line demonstrates the ability of Nampt to provide protective effects from oxidative stress in that specific cell line. However developing Nampt for treatment in vivo has the complication that various cell types interact with each other, versus tissue culture where Nampt is only targeting one cell type.

To address the role of Nampt in neuronal protection siRNA was used to knockdown endogenous Nampt. The use of siRNA would allow for the removal of NAMPT from cells and of all the proteins functions, not just inhibition of the active site



and depleting NAD<sup>+</sup> stores. During the experiments the limitation of using extracellular rNampt is having the same concentration of Nampt entering each cell via pinocytosis, and having each cell receive the same amount of Nampt is a difficult process, due to the cells ability to take up Nampt. To address this question the creation of a stable Nampt cell line under an inducible promotor could be constructed to control the expression of Nampt in each cell line. The generation of a vector with a short hair pin of RNAi could be created to use for the knockdown of Nampt and create a stable cell line. This could be done to ensure higher percentage knockdown of Nampt verses the use of siRNA where transfection was below 50

The use of SH-SY5Y cells allowed for testing using tBHP to induce oxidative stress and apoptosis to be seen in an in vitro model. With the addition of rNampt cell viability was seen to have significant protection from oxidative stress when tested with Calcein-AM assay. Testing of ARPE-19 cell treatment using rNampt to provide protection from oxidative stress damage showed that rNampt does prevent cells from entering apoptosis. Visual cell counts showed that significant cell survival was seen with the addition of rNampt. siRNA transfections demonstrated that the effects seen with rNampt as a protective agent is focused on the production of NMN for NAD production by the knockdown of endogenous NAMPT. Use of the ONHA cell line allowed for the testing of rNampt to prevent effects of oxidative stress in Glaucoma. Protection and cell survival was significantly increased when rNampt was present and cells were protected when endogenous NAMPT was knocked down. Indicating that neurodegenerative diseases that are caused by oxidative stress can be prevented by the addition of rNampt to prevent cell loss by apoptosis by NAD depletion.

Localization of protein NAMPT plays a key role on what beneficial effects the protein can exert upon the cell. Nampt as a cytokine has only been shown in B-cell maturation and inflammatory response. The cell lines used in this experiment have not been shown to have Nampt activity as a cytokine nor undergo an inflammatory response, indicating the protective effects observed are generated from the production of NAD<sup>+</sup>. Nampt is shown to be localized intracellular and extracellular and can convert NAM to NMN for NAD<sup>+</sup> biosynthesis. Conversion of NMN to NAD is performed by Nicotinamide mononucleotide adenylytransferase 1 (Nmnat), Nmnat1-3 are compartmentalized in the nucleus, cytoplasm, and mitochondria (91). Enabling NAD biosynthesis mediated by Nampt to take place in different compartments of the cell and provide more NAD<sup>+</sup> for cell survival.

## CHAPTER 5

### FUTURE DIRECTIONS

In the future it would be interesting to look at the role of sirtuins in this pathway and the effects they have on mitochondrial biogenesis. Since NAD<sup>+</sup> is required for the functions of sirtuins, via the conversion of NAD to cADPR and NAM, NAMPT-mediated NAD<sup>+</sup> biosynthesis might play an important role in regulating sirtuin activity (92). The decline in NAD<sup>+</sup> biosynthesis could be an important trigger for a variety of pathophysiological changes that contribute to aging through decreased activity of sirtuins. NAMPT-mediated NAD<sup>+</sup> biosynthesis declines with age, which might reduce sirtuin activity.

Nampt-NAD-SIRT cascade pathway has been used as a target point for stroke damage. Studies have shown that NAMPT can be a pleiotropic target and a source for therapeutic interventions in stroke models (93). The use of NAMPT targeting could be applied to neurodegenerative diseases and the potential of new therapeutic treatments in Alzheimer's disease and Glaucoma could be introduced.

## REFERENCES

1. Hebert LE, Weuve J, Scherr PA, Evans DL. 2013. Alzheimer disease in the United States estimated using the 2010 census. *Neurology* 80:1778-83
2. Klein R, Klein BE. 2013. The prevalence of age-related eye diseases and visual impairment in aging: current estimates. *Invest Ophthalmol Vis Sci* 54:ORSF5-ORSF13.
3. Kakizuka A. 2015. VCP, a Major ATPase in the Cells, as a Novel Drug Target for Currently Incurable Disorders, p 61-69. *In* Nakao K, Minato N, Uemoto S (ed), *Innovative Medicine: Basic Research and Development* doi:10.1007/978-4-431-55651-0\_5, Tokyo.
4. JPND Research. 2015. *What is Neurodegenerative Disease*. <http://www.neurodegenerationresearch.eu/about/what/>
5. Rubinsztein DC. 2006. The roles of intracellular protein-degradation pathways in neurodegeneration. *Nature* 443:780-6.
6. Engelberg-Kulka H, Amitai S, Kolodkin-Gal I, Hazan R. 2006. Bacterial programmed cell death and multicellular behavior in bacteria. *PLoS Genet* 2:e135.
7. Green DR. 2011. *Means to an End: Apoptosis and Other cell Death Mechanisms*. Cold Spring Harbor Laboratory Press.
8. DiMauro S, Schon EA. 2008. Mitochondrial disorders in the nervous system. *Annu Rev Neurosci* 31:91-123.
9. Masuda T, Shimazawa M, Hara H. 2017. Retinal Diseases Associated with Oxidative Stress and the Effects of a Free Radical Scavenger (Edaravone). *Oxid Med Cell Longev* 2017:9208489.
10. Prof Martin Prince PAW, Dr Maelenn Guerchet, Gemma-Clair Ali, Dr Yu-Tzu Wu, Dr matthew Prina. 2015. *World Alzheimer Report 2015*. ADI, International AsD, Alzheimer's Disease international.

11. Ferri CP, Prince M, Brayne C, Brodaty H, Fratiglioni L, Ganguli M, Hall K, Hasegawa K, Hendrie H, Huang Y, Jorm A, Mathers C, Menezes PR, Rimmer E, Scazufca M, Alzheimer's Disease I. 2005. Global prevalence of dementia: a Delphi consensus study. *Lancet* 366:2112-7.
12. Bekris LM, Yu CE, Bird TD, Tsuang DW. 2010. Genetics of Alzheimer disease. *J Geriatr Psychiatry Neurol* 23:213-27.
13. Braak H, Braak E. 1997. Frequency of stages of Alzheimer-related lesions in different age categories. *Neurobiol Aging* 18:351-7.
14. Goedert M, Spillantini MG. 2006. A century of Alzheimer's disease. *Science* 314:777-81.
15. Glenner GG, Wong CW, Quaranta V, Eanes ED. 1984. The amyloid deposits in Alzheimer's disease: their nature and pathogenesis. *Appl Pathol* 2:357-69.
16. Iwatsubo T, Odaka A, Suzuki N, Mizusawa H, Nukina N, Ihara Y. 1994. Visualization of A beta 42(43) and A beta 40 in senile plaques with end-specific A beta monoclonals: evidence that an initially deposited species is A beta 42(43). *Neuron* 13:45-53.
17. Mattson MP. 2004. Pathways towards and away from Alzheimer's disease. *Nature* 430:631-9.
18. Mattson MP. 2010. ER calcium and Alzheimer's disease: in a state of flux. *Sci Signal* 3:pe10.
19. Xu L, Eu JP, Meissner G, Stamler JS. 1998. Activation of the cardiac calcium release channel (ryanodine receptor) by poly-S-nitrosylation. *Science* 279:234-7.
20. Payne AJ, Gerdes BC, Naumchuk Y, McCalley AE, Kaja S, Koulen P. 2013. Presenilins regulate the cellular activity of ryanodine receptors differentially through isotype-specific N-terminal cysteines. *Exp Neurol* 250:143-50.
21. Izzotti A, Bagnis A, Sacca SC. 2006. The role of oxidative stress in glaucoma. *Mutat Res* 612:105-14.

22. Seki M, Lipton SA. 2008. Targeting excitotoxic/free radical signaling pathways for therapeutic intervention in glaucoma. *Prog Brain Res* 173:495-510.
23. Janssen SF, Gorgels TG, Ramdas WD, Klaver CC, van Duijn CM, Jansonius NM, Bergen AA. 2013. The vast complexity of primary open angle glaucoma: disease genes, risks, molecular mechanisms and pathobiology. *Prog Retin Eye Res* 37:31-67.
24. Osborne NN, del Olmo-Aguado S. 2013. Maintenance of retinal ganglion cell mitochondrial functions as a neuroprotective strategy in glaucoma. *Curr Opin Pharmacol* 13:16-22.
25. Shen F, Chen B, Danias J, Lee KC, Lee H, Su Y, Podos SM, Mittag TW. 2004. Glutamate-induced glutamine synthetase expression in retinal Muller cells after short-term ocular hypertension in the rat. *Invest Ophthalmol Vis Sci* 45:3107-12.
26. Galassi F, Renieri G, Sodi A, Ucci F, Vannozzi L, Masini E. 2004. Nitric oxide proxies and ocular perfusion pressure in primary open angle glaucoma. *Br J Ophthalmol* 88:757-60.
27. Chung HS, Harris A, Evans DW, Kagemann L, Garzosi HJ, Martin B. 1999. Vascular aspects in the pathophysiology of glaucomatous optic neuropathy. *Surv Ophthalmol* 43 Suppl 1:S43-50.
28. Moreno MC, Campanelli J, Sande P, Sanz DA, Keller Sarmiento MI, Rosenstein RE. 2004. Retinal oxidative stress induced by high intraocular pressure. *Free Radic Biol Med* 37:803-12.
29. Alvarado J, Murphy C, Polansky J, Juster R. 1981. Age-related changes in trabecular meshwork cellularity. *Invest Ophthalmol Vis Sci* 21:714-27.
30. Alvarado J, Murphy C, Juster R. 1984. Trabecular meshwork cellularity in primary open-angle glaucoma and nonglaucomatous normals. *Ophthalmology* 91:564-79.
31. Sacca SC, Pascotto A, Camicione P, Capris P, Izzotti A. 2005. Oxidative DNA damage in the human trabecular meshwork: clinical correlation in patients with primary open-angle glaucoma. *Arch Ophthalmol* 123:458-63.

32. Chen JZ, Kadlubar FF. 2003. A new clue to glaucoma pathogenesis. *Am J Med* 114:697-8.
33. Truscott RJ. 2005. Age-related nuclear cataract-oxidation is the key. *Exp Eye Res* 80:709-25.
34. Yildirim O, Ates NA, Tamer L, Muslu N, Ercan B, Atik U, Kanik A. 2004. Changes in antioxidant enzyme activity and malondialdehyde level in patients with age-related macular degeneration. *Ophthalmologica* 218:202-6.
35. National Eye Institute. 2015. *Facts About Age-Related Macular Degeneration*. [https://nei.nih.gov/health/maculardegen/armd\\_facts](https://nei.nih.gov/health/maculardegen/armd_facts)
36. Bowes Rickman C, Farsiu S, Toth CA, Klingeborn M. 2013. Dry age-related macular degeneration: mechanisms, therapeutic targets, and imaging. *Invest Ophthalmol Vis Sci* 54:ORSF68-80.
37. Seddon M, Looi YH, Shah AM. 2007. Oxidative stress and redox signalling in cardiac hypertrophy and heart failure. *Heart* 93:903-7.
38. Barja G, Herrero A. 2000. Oxidative damage to mitochondrial DNA is inversely related to maximum life span in the heart and brain of mammals. *FASEB J* 14:312-8.
39. Samal B, Sun Y, Stearns G, Xie C, Suggs S, McNiece I. 1994. Cloning and characterization of the cDNA encoding a novel human pre-B-cell colony-enhancing factor. *Mol Cell Biol* 14:1431-7.
40. McGlothlin JR, Gao L, Lavoie T, Simon BA, Easley RB, Ma SF, Rumala BB, Garcia JG, Ye SQ. 2005. Molecular cloning and characterization of canine pre-B-cell colony-enhancing factor. *Biochem Genet* 43:127-41.
41. Ognjanovic S, Tashima LS, Bryant-Greenwood GD. 2003. The effects of pre-B-cell colony-enhancing factor on the human fetal membranes by microarray analysis. *Am J Obstet Gynecol* 189:1187-95.
42. Brower RG. 2002. Mechanical ventilation in acute lung injury and ARDS. Tidal volume reduction. *Crit Care Clin* 18:1-13, v.

43. Groeneveld AB. 2002. Vascular pharmacology of acute lung injury and acute respiratory distress syndrome. *Vascul Pharmacol* 39:247-56.
44. Ramsey KM, Yoshino J, Brace CS, Abrassart D, Kobayashi Y, Marcheva B, Hong HK, Chong JL, Buhr ED, Lee C, Takahashi JS, Imai S, Bass J. 2009. Circadian clock feedback cycle through NAMPT-mediated NAD<sup>+</sup> biosynthesis. *Science* 324:651-4.
45. Dirnagl U, Iadecola C, Moskowitz MA. 1999. Pathobiology of ischaemic stroke: an integrated view. *Trends Neurosci* 22:391-7.
46. Yang H, Yang T, Baur JA, Perez E, Matsui T, Carmona JJ, Lamming DW, Souza-Pinto NC, Bohr VA, Rosenzweig A, de Cabo R, Sauve AA, Sinclair DA. 2007. Nutrient-sensitive mitochondrial NAD<sup>+</sup> levels dictate cell survival. *Cell* 130:1095-107.
47. Berridge MJ, Bootman MD, Roderick HL. 2003. Calcium signalling: dynamics, homeostasis and remodelling. *Nat Rev Mol Cell Biol* 4:517-29.
48. Koulen P, Thrower EC. 2001. Pharmacological modulation of intracellular Ca<sup>2+</sup> channels at the single-channel level. *Mol Neurobiol* 24:65-86.
49. Akpınar A, Uguz AC, Naziroglu M. 2014. Agomelatine and duloxetine synergistically modulates apoptotic pathway by inhibiting oxidative stress triggered intracellular calcium entry in neuronal PC12 cells: role of TRPM2 and voltage-gated calcium channels. *J Membr Biol* 247:451-9.
50. Wiederkehr A, Park KS, Dupont O, Demaurex N, Pozzan T, Cline GW, Wollheim CB. 2009. Matrix alkalization: a novel mitochondrial signal for sustained pancreatic beta-cell activation. *EMBO J* 28:417-28.
51. Tarasov AI, Semplici F, Ravier MA, Bellomo EA, Pullen TJ, Gilon P, Sekler I, Rizzuto R, Rutter GA. 2012. The mitochondrial Ca<sup>2+</sup> uniporter MCU is essential for glucose-induced ATP increases in pancreatic beta-cells. *PLoS One* 7:e39722.
52. Jouaville LS, Pinton P, Bastianutto C, Rutter GA, Rizzuto R. 1999. Regulation of mitochondrial ATP synthesis by calcium: evidence for a long-term metabolic priming. *Proc Natl Acad Sci U S A* 96:13807-12.



53. Denton RM. 2009. Regulation of mitochondrial dehydrogenases by calcium ions. *Biochim Biophys Acta* 1787:1309-16.
54. Berridge MJ, Bootman MD, Lipp P. 1998. Calcium--a life and death signal. *Nature* 395:645-8.
55. Petersen OH, Petersen CC, Kasai H. 1994. Calcium and hormone action. *Annu Rev Physiol* 56:297-319.
56. Clapham DE. 1995. Calcium signaling. *Cell* 80:259-68.
57. Berridge MJ. 1998. Neuronal calcium signaling. *Neuron* 21:13-26.
58. Bootman MD, Collins TJ, Peppiatt CM, Prothero LS, MacKenzie L, De Smet P, Travers M, Tovey SC, Seo JT, Berridge MJ, Ciccolini F, Lipp P. 2001. Calcium signalling--an overview. *Semin Cell Dev Biol* 12:3-10.
59. Orrenius S, Zhivotovsky B, Nicotera P. 2003. Regulation of cell death: the calcium-apoptosis link. *Nat Rev Mol Cell Biol* 4:552-65.
60. Fleckenstein A, Janke J, Doring HJ, Leder O. 1974. Myocardial fiber necrosis due to intracellular Ca overload-a new principle in cardiac pathophysiology. *Recent Adv Stud Cardiac Struct Metab* 4:563-80.
61. Bose T, Cieslar-Pobuda A, Wiechec E. 2015. Role of ion channels in regulating Ca(2)(+) homeostasis during the interplay between immune and cancer cells. *Cell Death Dis* 6:e1648.
62. Wosikowski K, Mattern K, Schemainda I, Hasmann M, Rattel B, Loser R. 2002. WK175, a novel antitumor agent, decreases the intracellular nicotinamide adenine dinucleotide concentration and induces the apoptotic cascade in human leukemia cells. *Cancer Res* 62:1057-62.
63. Martinsson P, de la Torre M, Binderup L, Nygren P, Larsson R. 2001. Cell death with atypical features induced by the novel antitumoral drug CHS 828, in human U-937 GTB cells. *Eur J Pharmacol* 417:181-7.

64. Tan B, Young DA, Lu ZH, Wang T, Meier TI, Shepard RL, Roth K, Zhai Y, Huss K, Kuo MS, Gillig J, Parthasarathy S, Burkholder TP, Smith MC, Geeganage S, Zhao G. 2013. Pharmacological inhibition of nicotinamide phosphoribosyltransferase (NAMPT), an enzyme essential for NAD<sup>+</sup> biosynthesis, in human cancer cells: metabolic basis and potential clinical implications. *J Biol Chem* 288:3500-11.
65. Magnone M, Bauer I, Poggi A, Mannino E, Sturla L, Brini M, Zocchi E, De Flora A, Nencioni A, Bruzzone S. 2012. NAD<sup>+</sup> levels control Ca<sup>2+</sup> store replenishment and mitogen-induced increase of cytosolic Ca<sup>2+</sup> by Cyclic ADP-ribose-dependent TRPM2 channel gating in human T lymphocytes. *J Biol Chem* 287:21067-81.
66. Takeuchi M, Yamamoto T. 2015. Apoptosis induced by NAD depletion is inhibited by KN-93 in a CaMKII-independent manner. *Exp Cell Res* 335:62-7.
67. Huber A, Stuchbury G, Burkle A, Burnell J, Munch G. 2006. Neuroprotective therapies for Alzheimer's disease. *Curr Pharm Des* 12:705-17.
68. Yu YC, Kuo CL, Cheng WL, Liu CS, Hsieh M. 2009. Decreased antioxidant enzyme activity and increased mitochondrial DNA damage in cellular models of Machado-Joseph disease. *J Neurosci Res* 87:1884-91.
69. Zuo L, Motherwell MS. 2013. The impact of reactive oxygen species and genetic mitochondrial mutations in Parkinson's disease. *Gene* 532:18-23.
70. Kim GH, Kim JE, Rhie SJ, Yoon S. 2015. The Role of Oxidative Stress in Neurodegenerative Diseases. *Exp Neurobiol* 24:325-40.
71. Cobb CA, Cole MP. 2015. Oxidative and nitrative stress in neurodegeneration. *Neurobiol Dis* doi:10.1016/j.nbd.2015.04.020.
72. Hayashi M. 2009. Oxidative stress in developmental brain disorders. *Neuropathology* 29:1-8.
73. Sultana R, Perluigi M, Allan Butterfield D. 2013. Lipid peroxidation triggers neurodegeneration: a redox proteomics view into the Alzheimer disease brain. *Free Radic Biol Med* 62:157-69.

74. Gandhi S, Abramov AY. 2012. Mechanism of oxidative stress in neurodegeneration. *Oxid Med Cell Longev* 2012:428010.
75. Federico A, Cardaioli E, Da Pozzo P, Formichi P, Gallus GN, Radi E. 2012. Mitochondria, oxidative stress and neurodegeneration. *J Neurol Sci* 322:254-62.
76. Patten DA, Germain M, Kelly MA, Slack RS. 2010. Reactive oxygen species: stuck in the middle of neurodegeneration. *J Alzheimers Dis* 20 Suppl 2:S357-67.
77. Kaja S, Duncan RS, Longoria S, Hilgenberg JD, Payne AJ, Desai NM, Parikh RA, Burroughs SL, Gregg EV, Goad DL, Koulen P. 2011. Novel mechanism of increased Ca<sup>2+</sup> release following oxidative stress in neuronal cells involves type 2 inositol-1,4,5-trisphosphate receptors. *Neuroscience* 175:281-91.
78. Tseng PL, Chen CW, Hu KH, Cheng HC, Lin YH, Tsai WH, Cheng TJ, Wu WH, Yeh CW, Lin CC, Tsai HJ, Chang HC, Chuang JH, Shan YS, Chang WT. 2018. The decrease of glycolytic enzyme hexokinase 1 accelerates tumor malignancy via deregulating energy metabolism but sensitizes cancer cells to 2-deoxyglucose inhibition. *Oncotarget* 9:18949-18969.
79. Kaja S, Payne AJ, Naumchuk Y, Levy D, Zaidi DH, Altman AM, Nawazish S, Ghuman JK, Gerdes BC, Moore MA, Koulen P. 2015. Plate reader-based cell viability assays for glioprotection using primary rat optic nerve head astrocytes. *Exp Eye Res* 138:159-66.
80. Burroughs SL, Duncan RS, Rayudu P, Kandula P, Payne AJ, Clark JL, Koulen P, Kaja S. 2012. Plate reader-based assays for measuring cell viability, neuroprotection and calcium in primary neuronal cultures. *J Neurosci Methods* 203:141-5.
81. BioResearch. Amaxa 4D-Nucleofector Protocol for Normal Human Bronchial Epithelial Cells.
82. Kaarniranta K, Salminen A, Haapasalo A, Soininen H, Hiltunen M. 2011. Age-related macular degeneration (AMD): Alzheimer's disease in the eye? *J Alzheimers Dis* 24:615-31.
83. Zhang HS, Sang WW, Wang YO, Liu W. 2010. Nicotinamide phosphoribosyltransferase/sirtuin 1 pathway is involved in human

- immunodeficiency virus type 1 Tat-mediated long terminal repeat transactivation. *J Cell Biochem* 110:1464-70.
84. Wang F, Zhang WP. 2011. [Research progress on nicotinamide phosphoribosyl transferase involved in aging and age-related diseases]. *Zhejiang Da Xue Xue Bao Yi Xue Ban* 40:680-4.
  85. Stein LR, Wozniak DF, Dearborn JT, Kubota S, Apte RS, Izumi Y, Zorumski CF, Imai S. 2014. Expression of Nampt in hippocampal and cortical excitatory neurons is critical for cognitive function. *J Neurosci* 34:5800-15.
  86. Lin JB, Kubota S, Ban N, Yoshida M, Santeford A, Sene A, Nakamura R, Zapata N, Kubota M, Tsubota K, Yoshino J, Imai SI, Apte RS. 2016. NAMPT-Mediated NAD(+) Biosynthesis Is Essential for Vision In Mice. *Cell Rep* 17:69-85.
  87. Canto C, Menzies KJ, Auwerx J. 2015. NAD(+) Metabolism and the Control of Energy Homeostasis: A Balancing Act between Mitochondria and the Nucleus. *Cell Metab* 22:31-53.
  88. Lin JB, Apte RS. 2018. NAD(+) and sirtuins in retinal degenerative diseases: A look at future therapies. *Prog Retin Eye Res*  
doi:10.1016/j.preteyeres.2018.06.002.
  89. Schondorf DC, Ivanyuk D, Baden P, Sanchez-Martinez A, De Cicco S, Yu C, Giunta I, Schwarz LK, Di Napoli G, Panagiotakopoulou V, Nestel S, Keatinge M, Pruszek J, Bandmann O, Heimrich B, Gasser T, Whitworth AJ, Deleidi M. 2018. The NAD+ Precursor Nicotinamide Riboside Rescues Mitochondrial Defects and Neuronal Loss in iPSC and Fly Models of Parkinson's Disease. *Cell Rep* 23:2976-2988.
  90. Hsu CP, Oka S, Shao D, Hariharan N, Sadoshima J. 2009. Nicotinamide phosphoribosyltransferase regulates cell survival through NAD+ synthesis in cardiac myocytes. *Circ Res* 105:481-91.
  91. Imai S. 2009. Nicotinamide phosphoribosyltransferase (Nampt): a link between NAD biology, metabolism, and diseases. *Curr Pharm Des* 15:20-8.
  92. Anonymous. 2016. Sirtuins, 1 ed doi:10.1007/978-94-024-0962-8. Springer Netherlands.

93. Wang P, Miao CY. 2015. NAMPT as a Therapeutic Target against Stroke. *Trends Pharmacol Sci* 36:891-905.

## VITA

Bryan Christopher Gerdes was born in Ponca City, OK and moved to Salina, KS before the age of two, and graduated High School from Salina High School South in 2001. Bryan then went on to attend Kansas State University and graduated in 2006 with a Bachelor of Science in Biology. In 2008 a second Bachelor of Science was awarded from Kansas State University this time in Microbiology. Bryan was employed by Edenspace after graduating in 2008 as a Research Associate I. In August of 2011 Bryan moved to Kansas City to work for Dr. Peter Koulen and the Vision Research Center at University of Missouri Kansas City. In 2013 Bryan was able to enroll in University of Missouri Kansas City graduate program and received a Master of Science degree in Cell Biology and Biophysics in May of 2015. Bryan received a 2016/2017 University of Missouri-Kansas City, School of Graduate Studies Research Award for his Ph.D. thesis work.